The European Zoological Journal

ISSN: 2475-0263 (Online) Journal homepage: www.tandfonline.com/journals/tizo21

A new *Diaforobiotus* species (Tardigrada: eutardigrada: richtersiusidae) from the Mexican transition zone, described based on multiple lines of evidence

R. A. Flores-Romero, D. López-Sandoval, J. Vincenzi, M. Cesari, R. Guidetti, A. Dueñas-Cedillo, E. A. Ruiz & F. Armendariz-Toledano

To cite this article: R. A. Flores-Romero, D. López-Sandoval, J. Vincenzi, M. Cesari, R. Guidetti, A. Dueñas-Cedillo, E. A. Ruiz & F. Armendariz-Toledano (2025) A new *Diaforobiotus* species (Tardigrada: eutardigrada: richtersiusidae) from the Mexican transition zone, described based on multiple lines of evidence, The European Zoological Journal, 92:1, 1171-1196, DOI: 10.1080/24750263.2025.2548265

To link to this article: https://doi.org/10.1080/24750263.2025.2548265

THE EUROPEAN ZOOLOGICAL JOURNAL
2025, VOL. 92, NO. 1, 1171–1196
https://doi.org/10.1080/24750263.2025.2548265

A new *Diaforobiotus* species (Tardigrada: eutardigrada: richtersiusidae) from the Mexican transition zone, described based on multiple lines of evidence

R. A. Flores-Romero [a,b], D. López-Sandoval [a,c], J. Vincenzi [d], M. Cesari[d], R. Guidetti[d], A. Dueñas-Cedillo [e], E. A. Ruiz [f] and F. Armendariz-Toledano [b]

[a]Posgrado en Ciencias Biológicas, Universidad Nacional Autónoma de México (UNAM), Ciudad Universitaria, Mexico City, Mexico; [b]Colección Nacional de Insectos (CNIN), Departamento de Zoología, Instituto de Biología, Universidad Nacional Autónoma de México (UNAM), Ciudad Universitaria, Mexico City, Mexico; [c]Colección Nacional de Ácaros (CNAC), Departamento de Zoología, Instituto de Biología, Universidad Nacional Autónoma de México (UNAM), Ciudad Universitaria, Mexico City, Mexico; [d]Department of Life Sciences, University of Modena and Reggio Emilia, Modena, Italy; [e]Facultad de Ciencias Forestales, Universidad Autónoma de Nuevo León, Linares, México; [f]Departamento de Zoología, Escuela Nacional de Ciencias Biológicas, Instituto Politécnico Nacional, Ciudad de México, México

ABSTRACT

The genus *Diaforobiotus* was established to accommodate species formerly assigned to the genus *Macrobiotus* (family Macrobiotidae), and is now placed within the family Richtersiusidae. Currently, the genus includes five species, one of which—*Diaforobiotus islandicus*—has been recorded in Mexico. Although most of the country lacks studies focused on tardigrades, the Trans-Mexican Volcanic Belt (TMVB) is interesting since it is positioned between two major biogeographic regions (the Neotropical and the Nearctic) and it serves both as a transition zone and as a hotspot of endemism. In this work, a new tardigrade species, *Diaforobiotus quetzalcoatli* sp. nov., found in Mount Tlaloc (a locality belonging to the TMVB, in central Mexico) is described. This new species is supported and described with an integrative approach using light, confocal, and scanning electron microscopy, as well as DNA sequences of four molecular markers (COI, ITS-2, 18S rRNA, and 28S rRNA). Phylogenetic analyses revealed that *D. quetzalcoatli* sp. nov. is closely related to *Diaforobiotus occidentalis* from Canada, and species delimitation analyses based on COI and ITS2 markers provide strong evidence that Mexican specimens represent a sixth distinct species within *Diaforobiotus*.

ARTICLE HISTORY
Received 7 July 2025
Accepted 11 August 2025
First Publication
6 October 2025

KEYWORDS
Altitudinal gradient; *Diaforobiotus*; DNA barcoding; HotShot; phylogeny and species delimitation

Introduction

Tardigrades, or "water bears", are microscopic metazoans in the phylum Tardigrada, growing through moulting (Schill 2008). These organisms thrive in diverse environments, from marine habitats to high-altitude mountains. Their unique ability to enter cryptobiosis, a state of suspended animation, enables them to survive extreme conditions such as dehydration, freezing, and even a total vacuum (Heinis 1911; Beasley 1972; Nelson 1982; McInnes & Convey 2005; Michalczyk & Kaczmarek 2006; Guil et al. 2009).

The current taxonomic classification of this group primarily relies upon morphological characters—such as the body shape, the claw morphology, the structure of the buccopharyngeal apparatus, the cuticle ornamentation and appendages, and the egg ornamentation (Nichols et al. 2006)—as well as relatively short DNA sequences such as COI and ITS-2 (Jørgensen et al. 2018).

Research on this phylum in Mexico is growing; however, studies on this phylum remain limited, and to date, most publications have focused on species descriptions (Pérez-Pech et al. 2017; Moreno-Talamantes et al. 2019; Moreno-Talamantes et al. 2020; Dueñas-Cedillo et al. 2020). The first major contribution was made by Hoffman and Jiménez (1994), who compiled a genus-level checklist identifying 16 genera. This was followed by the first species-level checklist by Kaczmarek et al. (2011b). More recently, studies by Moreno-Talamantes et al. (2019) and

CONTACT F. Armendariz-Toledano farmendariztoledano@ib.unam.mx Colección Nacional de Insectos (CNIN), Departamento de Zoología, Instituto de Biología, Universidad Nacional Autónoma de México (UNAM), Ciudad Universitaria, 3er. Circuito Exterior S/N, Ciudad Universitaria Alcaldía Coyoacán, Ciudad de México, Mexico City 04510, Mexico

Supplemental data for this article can be accessed online at https://doi.org/10.1080/24750263.2025.2548265.

García-Román et al. (2022) expanded the knowledge on diversity, which in turn led to an updated record of 43 genera and 75 species in the country (Dueñas-Cedillo et al. 2024).

Since 2018, researchers from various Mexican institutions have been conducting a tardigrade inventory in the Mexican Transition zone (MTZ), focusing on the Trans-Mexican Volcanic Belt (TMVB) to document limnoterrestrial tardigrades in this region (Dueñas-Cedillo et al. 2020, 2021, 2024; García-Román et al. 2022; Amezcua-Martínez et al. 2025). The inventory aims to (1) create and annotate a list of tardigrade species in the MTZ, (2) assess the environmental factors affecting their distribution and diversity, and (3) discover and describe new species. The MTZ is a complex region that extends from the southwestern United States through Mexico and into parts of Central America, reaching as far south as Nicaragua. The MTZ is a biogeographical area where Neotropical and Nearctic biotas overlap. This convergence has given rise to a wide variety of ecosystems, shaped by significant climatic variation and multiple geographic conditions (Morrone 2010). Within the MTZ, the TMVB plays a key role in species diversification, endemism, and biogeographic transitions (Morrone 2005). Molded by a dynamic volcanic history, isolated habitats, diverse elevations, and a wide range of climates, this region has ideal conditions for biodiversity and driving evolutionary processes (Morrone 2010; also see Mastretta-Yanes et al. 2015). The TMVB's environmental diversity and high endemism make it a promising area for species discovery (Gámez et al. 2012), including tardigrades (Dueñas-Cedillo et al. 2020). These animals have been previously found in coniferous forests and alpine grasslands, thriving in humid, temperate, and cold conditions (Bartels & Nelson 2006, 2007; Dueñas-Cedillo et al. 2020, 2021, 2024; García-Román et al. 2022), highlighting the TMVB as a suitable region for discovering a high diversity of tardigrades in various microhabitats. Kaczmarek et al. (2011a) noted that altitude and humidity are key variables influencing the distribution of tardigrades, while Guil et al. (2009) observed that species preferences for different altitudes can lead to greater species richness. Additionally, Gąsiorek et al. (2021) suggested that tardigrade fauna is frequently associated with cold habitats, and that geographically restricted areas such as islands or mountain ranges like the TMVB can foster endemism. Given the role of the TMVB in promoting endemism and its understudied tardigrade diversity, this study reports the discovery and description of *Diaforobiotus quetzalcoatli* sp. nov. from Mount Tlaloc, the ninth highest volcano in Mexico, which is located within the TMVB.

The genus *Diaforobiotus* was established by Guidetti et al. (2016), from species previously assigned to *Macrobiotus* (Macrobiotidae), and transferred to the family Richtersiusidae based on morphological and genetic evidence. The taxonomic history of this genus exemplifies the change of scientific understanding in response to new data and methodologies: since the initial description of the type species, it has undergone substantial taxonomic revisions, reflecting advances in integrative taxonomy and molecular methodologies (Murray 1910; Séméria 1985; Kathman 1990; Guidetti et al. 2016; Stec 2023; Massa et al. 2024). *Diaforobiotus* is a genus with five species, one of them with two subspecies (Degma & Guidetti 2024), mostly found in Europe (Richters 1904; Murray 1910; Maucci 1982; Kathman 1990; Stec & Morek 2022; Stec 2023). In Mexico, the only documented record of the family and genus is *D. islandicus* from Nuevo León (Moreno-Talamantes & León-Espinosa 2019); however, all records outside Iceland should be interpreted with caution (Stec 2023).

In this study, a population of *Diaforobiotus* was examined in Mount Tlaloc. Using an integrative approach that combines morphometry, phase contrast light microscopy (PCM) and scanning electron microscopy (SEM) imaging, as well as molecular evidence, *Diaforobiotus quetzalcoatli* sp. nov. was supported and described.

Materials and methods

Sampling

Mount Tlaloc is an inactive volcano located in Mexico state (in the central part of the country) (Figure 1). The combination of coniferous forest, alpine grassland, and nival zone, along with its volcanic origin and elevation gradient (1500–4150 m a.s.l.), provides an ideal microhabitat for tardigrades, aligning with previous findings on altitude-driven diversity (Bartels & Nelson 2006, 2007; Guil et al. 2009; Kaczmarek et al. 2011a; Gąsiorek et al. 2021). Specimens were obtained in the alpine grassland from three moss samples (4 cm^2 each) collected on rock at the southwest slope at 4037 m a.s.l., 19°24′46.1″N, 98°43′05.2″W, based on the WGS84 geographic reference system. The mosses were stored inside paper bags and dried.

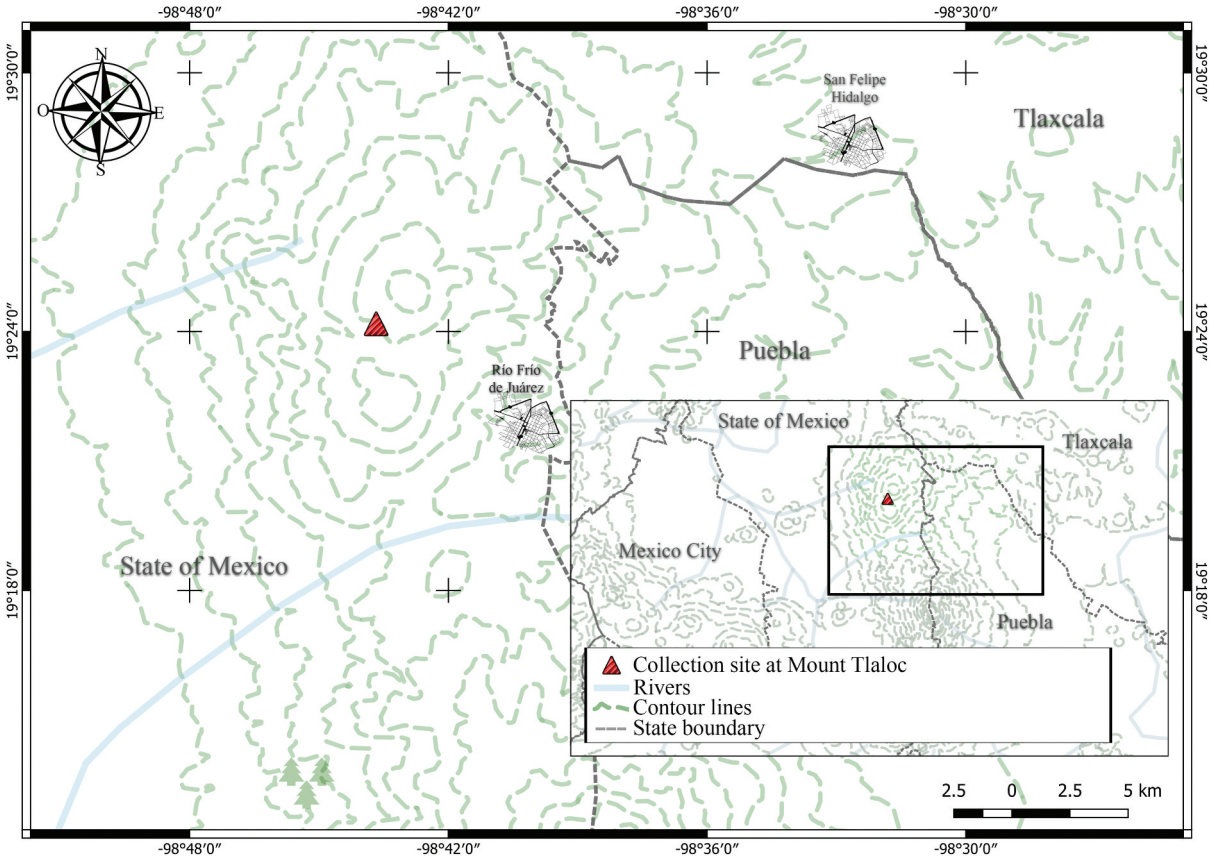

Figure 1. Geographic map indicating the type locality of *Diaforobiotus quetzalcoatli* sp. nov. in Mount Tlaloc, State of Mexico, Mexico.

Tardigrade processing

In the laboratory, a 2 g sample was taken from each collected moss and hydrated overnight. The samples were then shaken, and the water was filtered through a coarse sieve. Subsequently, the water was conducted through a series of mesh filters (500, 250, 74, and 24 µm), allowing tardigrades and their eggs to be retained on the meshes. Each supernatant was conducted through the sieves twice (double filtration) to obtain the largest number of specimens. Then, the moss was placed in a partially covered Petri dish at room temperature to dry for a week, and placed back in a paper bag.

Mounting and microscopy

To generate a series of preserved organisms that supports the identification used for the molecular analysis ("photogenophores" or "vouchers"), the specimens isolated from moss samples were divided equally into three subsamples: the first one for the paragenophores (specimens sampled at the same time and locality as the ones used for molecular analyses), the second one for the gDNA extractions, and the third one for SEM. Paragenophores were mounted on slides with polyvinyl lactophenol (PVA) and Hoyer medium. Specimens intended for gDNA extraction were individually mounted on cavity slides using a drop of water as the mounting medium for provisional preparations (modified from Amezcua-Martínez et al. 2025). Specimens for SEM were prepared according to Camarda et al. (2023). Both provisional and permanent slides were observed and photographed at different magnifications (10×, 20×, 40×, and 100×) by PCM using a Zeiss Axioskop with AxioCam ERc 5s digital camera. The measurements were taken using the program ImageJ (Schneider et al. 2012). Specimens for SEM were examined in a Hitachi model SU 1510 scanning electron microscope. All the images were obtained at the Laboratorio de Botánica Estructural and the Laboratorio de

Microscopía y Fotografía de la Biodiversidad I of the Instituto de Biología, Universidad Nacional Autónoma de México (UNAM), both part of the Laboratorio Nacional de la Biodiversidad (LaNaBio).

Identification, morphometry, and morphological nomenclature

Specimens were identified using the taxonomic key by Pilato and Binda (2010). The specimens were compared with other *Diaforobiotus* species using the keys of Stec (2023) and Massa et al. (2024).

The sample size for morphometrics was chosen following recommendations by Stec et al. (2016). All measurements were made in micrometres (µm). The terminology of the buccopharyngeal apparatus and claws was based on Pilato and Binda (2010). The claw measurements were taken according to Kaczmarek and Michalczyk (2017). The macroplacoid length sequence was determined according to Kaczmarek et al. (2014b). Ventral and dorsal cuticular pores were measured (the raw morphometric data are provided in SM.01). Morphometric data were managed using the template "Parachela" v. 1.2, available in the Tardigrada Register (Michalczyk & Kaczmarek 2013).

Moss identification

The mosses were identified using the key by Delgadillo-Moya et al. (2022). To analyse the distribution and shape of the leaves, the moss stem was observed under a Stemi 2000-C stereoscopic microscope, and an Axiolab Zeiss bright field microscope. The sporophyte and gametophyte were prepared for the histological section. Furthermore, the moss was identified through the specific DNA marker rbcL coding region within the chloroplast, for large subunit ribulose-1,5-bisphosphate carboxylase/oxygenase (RuBisCo) (Fazekas et al. 2012). The gametophyte with green leaves was extracted (without rhizoids) and washed with distilled water. Subsequently, the moss sample was macerated in a microtube, frozen in liquid nitrogen, and then subjected to cell disruption using a TissueLyser (method modified from Dellaporta et al. 1983). For DNA extraction, a FavorPrep Plant Genomic DNA Extraction Mini Kit (FAPGK001) (FavorGen Biotech Corp) was used. The primers and sources for amplification are listed in Table 1.

DNA sequencing for tardigrades

To confirm identification and to take photographs of taxonomically relevant structures such as the buccopharyngeal apparatus, claws, and cuticles, before DNA extraction, specimens were mounted in water on cavity slides and examined under PCM using a Zeiss Axioskop microscope. Subsequently, the photographed specimens (photogenophores) were processed for DNA extraction. The HotShot technique (Montero-Pau et al. 2008; Amezcua-Martínez et al. 2025) was employed for DNA extraction, because it is a fast, economical, and efficient method for obtaining tardigrade gDNA. We amplified fragments of the the small and large ribosomal subunits (18S rRNA and 28S rRNA), the internal transcribed spacer (ITS-2) and the cytochrome C oxidase subunit I (COI). Primers and Polymerase Chain Reaction (PCR) programmes for amplification are listed in Table 2. The PCR products were

Table 1. DNA markers and primers used for identification of mosses using the unit RuBisCo.

DNA marker	Primer direction	Primer sequence (5″–3″)	Source
rbclaF +634-F	Forward	5′-ATGTCACCACAAACAGAGACTAAAGC- 3′	Fazekas et al. (2012)
rbclaF +634-R	Reverse	5′ -GAAACGGTCTCTCCAACGCAT –3′	

Table 2. DNA markers and primers employed for amplification and sequencing of DNA fragments of *Diaforobiotus quetzalcoatli* sp. nov.

DNA marker	Primer name	Primer direction	Primer sequence (5″–3″)	Source	PCR programme
Small Sub-Unit ribosomal Ribonucleic Acid (18SrRNA)	18S_Tar_1Ff	Forward	AGGCGAAACCGCGAATGGCTC	Stec et al. (2017)	Stec et al. (2020a)
	18S_Tar_1Rr	Reverse	GCCGCAGGCTCCACTCCTGG		
Large Sub-Unit ribosomal Ribonucleic (28SrRNA)	28S_Eutar_F	Forward	ACCCGCTGAACTTAAGCATAT	Gąsiorek et al. (2018)	Stec et al. (2020a)
	28SR0990	Reverse	CCTTGGTCCGTGTTTCAAGAC	Mironov et al. (2012)	
Internal Transcribed Spacer 2 (ITS-2)	ITS2_Eutar_Ff	Forward	CGTAACGTGAATTGCAGGAC	Stec et al. (2018)	Stec et al. (2020a)
	ITS2_Eutar_Rr	Reverse	TCCTCCGCTTATTGATATGC		
Cytochrome C Oxidase subunit I (COI)	LCO1490	Forward	GGTCAACAAATCATAAAGATATTGG	Folmer et al. (1994)	Michalczyk et al. (2012)
	HCO2198	Reverse	TAAACTTCAGGGTGACCAAAAAATCA		

corroborated by 1.5% agarose gel electrophoresis stained with GelRed Nucleic Acid Gel Stain 10,000× (Biotium™) and purified with the ExoSap-IT enzyme (Applied Biosystems), following the manufacturer's instructions. The sequence reaction was prepared with 4 µL of water, 2 µL of Buffer 5×, 2 µL of big dye Terminator v. 3.1 (Applied Biosystems), 1 µL of the primer, and 2.5 µL of purified product. The reaction was placed in a PCR 2720 according to Amezcua-Martínez et al. (2025). When finished, samples were purified with Sephadex CentriSep™ plates (Princeton) and read in a 3730xl sequencer (Applied Biosystems) at the LaNaBio.

Phylogenetic analyses and genetic delimitation of the new species

Newly generated sequences were analysed using the programs FINCH TV (Geospiza, Inc 2004) and MEGA11 (Tamura et al. 2021). The identity of the obtained sequences was verified using BLAST (Altschul et al. 1990). As support for the phenotypic differential diagnosis between the new species and other *Diaforobiotus* species, marker sequences deposited in the GenBank database were used to calculate the uncorrected genetic distances (p-distance), using the program MEGA11 (Tamura et al. 2021). The *Diaforobiotus* species with sequences deposited in the GenBank database and used in this analysis are the following: *D. islandicus* (Richters, 1904), *D. occidentalis* (Murray, 1910), *D. hyperonix* (Maucci, 1982), and *D. svalbardicus* Stec, 2023. The distance matrices are provided in the Supplementary material (SM.02).

Phylogenetic analysis

To establish the phyletic position of the new species, a phylogenetic tree was constructed using the concatenated 18S rRNA + 28S rRNA + ITS-2 + COI sequences of the genus *Diaforobiotus* with the sequences of *Macrobiotus hannae* and *M. shonaicus* as outgroup (accession numbers are listed in Table 3). Sequences of

Table 3. List of species and their GenBank accession numbers for the nucleotide sequences used in the phylogenetic and genetic species delineation analyses (n/a = not available). New sequences are marked in bold.

Taxon	18s rRNA	28s rRNA	COI	ITS-2	Source
Diaforobiotus hyperonyx IT.339	OM179853	OM179860	OM151287	OM179866	Stec and Morek (2022)
Diaforobiotus hyperonyx IT.341	OM179855	OM179861	OM151288	OM179868	Stec and Morek (2022)
Diaforobiotus hyperonyx IT.344	OM179852	OM179859	OM151286	OM179867	Stec and Morek (2022)
Diaforobiotus hyperonyx IT.345	OM179854	OM179862	OM151289	OM179869	Stec and Morek (2022)
Diaforobiotus islandicus 1	HQ604972	n/a	n/a	n/a	Bertolani et al. (2014)
Diaforobiotus islandicus 2	HQ604973	n/a	n/a	n/a	Bertolani et al. (2014)
Diaforobiotus islandicus IS.042	MT812470	MT812461	MT808072	MT812597	Stec et al. (2020)
Diaforobiotus occidentalis S2011.Dia.V01	OQ029309	n/a	OQ029491	n/a	Massa et al. (2024)
Diaforobiotus occidentalis S2011.Dia.V02	OQ029310	n/a	OQ029492	n/a	Massa et al. (2024)
Diaforobiotus quetzalcoatli sp. nov. MT.MX.01	PV018904	n/a	PQ506034	PV018916	Present study
Diaforobiotus quetzalcoatli sp. nov. MT.MX.05	PV018905	PV018909	n/a	PV018917	Present study
Diaforobiotus quetzalcoatli sp. nov. MT.MX.06	n/a	PV018910	PQ506035	n/a	Present study
Diaforobiotus quetzalcoatli sp. nov. MT.MX.07	n/a	PV018911	n/a	PV018918	Present study
Diaforobiotus quetzalcoatli sp. nov. MT.MX.16	n/a	PV018912	n/a	n/a	Present study
Diaforobiotus quetzalcoatli sp. nov. MT.MX.17	n/a	n/a	PV017055	PV018919	Present study
Diaforobiotus quetzalcoatli sp. nov. MT.MX.19	n/a	n/a	n/a	PV018920	Present study
Diaforobiotus quetzalcoatli sp. nov. MT.MX.26	PV018906	PV018913	PV017056	n/a	Present study
Diaforobiotus quetzalcoatli sp. nov. MT.MX.30	PV018907	PV018914	PV017057	PV018921	Present study
Diaforobiotus quetzalcoatli sp. nov. MT.MX.33	PV018908	PV018915	PV017058	PV018922	Present study
Diaforobiotus quetzalcoatli sp. nov. MT.MX.34	n/a			PV018923	Present study
Diaforobiotus svalbardicus NO.386	MT812471	MT812463	MT808074	MT812598	Stec et al. (2020b)
Diaforobiotus sp. ID.517	MT812472	MT812462	MT808073	MT812599	Stec et al. (2020b)
Richtersius coronifer NO.385	MH681760	MH681757	MH676053	MH681763	Stec et al. (2020a)
Richtersius aff. *coronifer* IT.120	MH681761	MH681758	MH676054	MH681764	Stec et al. (2020a)
Richtersius aff. *coronifer* IT.317 1	MK211387	MK211385	MK214326	MK211382	Stec et al. (2020a)
Richtersius aff. *coronifer* IT.317 2	n/a	n/a	MK214327	MK211383	Stec et al. (2020a)
Richtersius aff. *coronifer* IT.317 3	n/a	n/a	MK214328	n/a	Stec et al. (2020a)
Richtersius aff. *coronifer* PL.247	MH681762	MH681759	MH676055	MH681765	Stec et al. (2020a)
Richtersius tertius GR.008 1	MK211386	MK211384	MK214323	MK211380	Stec et al. (2020a); Pogwizd and Stec (2022)
Richtersius tertius GR.008 2	n/a	n/a	MK214324	MK211381	Stec et al. (2020a); Pogwizd and Stec (2022)
Richtersius tertius GR.008 3	n/a	n/a	MK214325	n/a	Stec et al. (2020a); Pogwizd and Stec (2022)
Richtersius ziemowiti	MT241891	MT241895	MT246504	MT241896	Kayastha et al. (2020)
Macrobiotus hannae	MH063922	MH063924	MH057764	MH063923	Nowak and Stec (2018)
Macrobiotus shonaicus	MG757132	MG757133	MG757136	MG757134	Stec et al. (2018)

the newly barcoded species and sequences of species obtained from GenBank were aligned with the MAFFT algorithm version 7 (Katoh et al. 2002) implemented in the MAFFT online service (Katoh et al. 2019). Sequences were checked by visual inspection and translated to amino acids using the invertebrate mitochondrial code implemented in MEGA11 (Tamura et al. 2021) to check for the presence of pseudogenes. The sequences were concatenated using SequenceMatrix (Vaidya et al. 2011). The concatenated alignment was divided into six data blocks, constituting three separate blocks of ribosomal markers and three separate blocks of three codon positions in the COI data set. We selected the best partitioning scheme with the program ModelFinder (Kalyaanamoorthy et al. 2017) and the best substitution model for the posterior phylogenetic analysis using ModelTest-NG (Darriba et al. 2020). The optimal substitution model for each partition, identified using the Bayesian Information Criterion (BIC), was as follows: HKY+G4 for the first codon position of COI, GTR+I+G4 for the third codon position of COI, and GTR+G4 for the second codon position of COI, as well as for the datasets of 28S, 18S, and ITS-2. Bayesian inference (BI) marginal posterior probabilities were estimated using MrBayes v. 3.2 (Ronquist & Huelsenbeck 2003). The analysis was run for 10 million generations, starting from random trees, with the Markov chain sampled every 1000 generations. The convergence between the two independent runs was confirmed by an average standard deviation of split frequencies below 0.01. To assess stationarity and determine the appropriate burn-in (set to the first 10% of generations), Tracer v. 1.7 (Rambaut et al. 2018) was used. Effective sample size (ESS) values exceeded 200, and the consensus tree was generated by summarizing the remaining topologies after excluding the burn-in. Additionally, maximum likelihood (ML) analyses were performed with IQ-TREE2 (Minh et al. 2020), and branch support values for the ML tree were calculated using 1000 ultrafast bootstrap replicates (UFBoot) (Hoang et al. 2018). The final consensus trees were visualized in FigTree v. 1.4.4, available at http://tree.bio.ed.ac.uk/software/figtree, and edited with Adobe Photoshop™ 2024.

Species delimitation

Putative species were inferred using COI and ITS-2 sequences through three different approaches: Poisson Tree Processes (PTP; Zhang et al. 2013), Assemble Species by Automatic Partitioning (ASAP; Puillandre et al. 2020), and haplotype/sequence parsimony network analysis. All three analyses were performed for COI, while only ASAP and network analyses were conducted for ITS-2.

The molecular analysis of the COI gene was conducted on a 648 bp dataset comprising 15 sequences, including six sequences from Mexico obtained in the present study and nine sequences retrieved from GenBank, representing congeneric taxa within the genus *Diaforobiotus*. The ITS-2 fragment was analysed using a dataset of 450 bp, composed of eight sequences obtained from Mexican specimens and seven sequences retrieved from GenBank, except for *Diaforobiotus occidentalis*, for which ITS-2 sequences were not available (accession numbers are listed in Table 3).

Pairwise genetic distances for COI and ITS2 were computed using MEGA11 for all sequences obtained for the present study and available *Diaforobiotus* sequences present in GenBank. *Macrobiotus shonaicus* Stec et al. 2018 (Eutardigrada, Macrobiotoidea; GenBank acc. n. MK757136) was used as an outgroup. Parsimony network relationships among specimens were inferred following the method described by Templeton et al. (1992), implemented in TCS v. 1.21 (Clement et al. 2000), and visualized using tcsBU (Múrias dos Santos et al. 2016). A 95% connection limit was applied, as recommended for species delimitation and discovery (Hart & Sunday 2007). Distance-based ASAP analysis was conducted on the online platform (https://bioinfo.mnhn.fr/abi/public/asap/). PTP analysis was performed using ML gene trees generated in RAxML version 8.2.12 (Stamatakis 2014) as implemented in CIPRES, utilizing GTR+G as the evolutionary model.

Comparative material

The new species was compared with the original descriptions and redescriptions of all currently known *Diaforobiotus* species and other useful literature: Richters (1904), Murray (1910), Maucci (1983), Séméria (1985), Kathman (1990), Stec and Morek (2022), Stec (2023), and Massa et al. (2024). Additionally, we examined the following type material (animals and eggs): *Diaforobiotus islandicus* (Slides 1680, 3026), *Diaforobiotus hyperonyx* (Slides 9980.95–9986.95) and *Macrobiotus ruffoi* (Slides 1342, 4132), deposited at

the Bertolani collection (University of Modena and Reggio Emilia, Italy) and Maucci collection (Natural History Museum of Verona, Italy).

Results

Taxonomic account

Phylum Tardigrada Doyère, 1840

Class Eutardigrada Richters, 1926

Order Parachela Schuster, Nelson, Grigarick and Christenberry, 1980

Family Richtersiusidae Guidetti, Schill, Giovannini, Massa, Goldoni, Ebel, Förschler, Rebecchi and Cesari, 2021

Diagnosis (amended by Massa et al. 2024)

Double claws Y-shaped, two branches with an evident common tract with different length, and an internal septum. Lunules I–III can be smooth or indented. Claws IV with an indented lunule, showing variability in the shape of the lunules. Buccal tube with ventral lamina presents, with a ventral thickening in its anterior portion and a cuticular thickening on the anterior, dorsal wall of the buccal tube (which can form a large apophysis). Transverse crest in the buccal armature absent. The pharynx contains two rounded macroplacoids. The presence of a microplacoid is variable, as it may be present or absent. Cuticular pores are observed in at least one life stage. Eggs are laid freely, exhibiting elongated conical processes and lacking areolation on the surface. Granulation on the body and legs is absent in all currently recognized species.

Genus *Diaforobiotus* Guidetti, Rebecchi, Bertolani, Jönsson, Kristensen and Cesari, 2016

Diagnosis (amended by Guidetti et al. 2016)

Eyes are present in all the species reported. Live animals are orange, yellow, or green; after mounting, they are transparent. The cuticle is smooth, with circular or elliptical pores present randomly scattered throughout the body. Relatively short buccopharyngeal apparatus, buccal tube rigid, 10 peribuccal lamellae, and ventral lamina are present. A dorsal thickening in the anterior portion of the buccal tube is present, in conjunction with a large tooth on the surface of the tube. The oral cavity armature is composed of three bands of teeth of different shapes. Posterior to the second band of teeth, several strong, scattered, round teeth are present. The first band is positioned posteriorly to the peribuccal lamellae, the second band with rows of granular teeth (larger than the first band), the third band composed of three large teeth, two lateral and a posterior medial tooth. Pharynx with triangular apophyses and two macroplacoids, rounded at the ends. Microplacoid may be present. Pulvinus can be present or absent in legs I–III on the internal surface. Richersiusidae type claws, with accessory points on primary branches. Legs I–III possess trapezoidal or rounded lunules, with teeth that may be present or absent. Claw IV features a large lunule bearing teeth of variable size and number. Eggs are laid freely, spherical with elongated conical processes, smooth egg surface without areolation or reticulation, and pores may be present or absent.

Diaforobiotus quetzalcoatli sp. nov.

Figures 2–8, Tables 4–6

Zoobank register number: urn:lsid:zoobank.org:pub:C28DDD5A-64A8-433D-8C80-50B49EED0D88

Material examined

Holotype, 22 paratypes, and three eggs on slides with Hoyer and PVA mounting media; six paratypes, identified as photogenophores (voucher specimens), were used for DNA extraction. Additionally, 10 paratypes and five eggs were prepared for SEM.

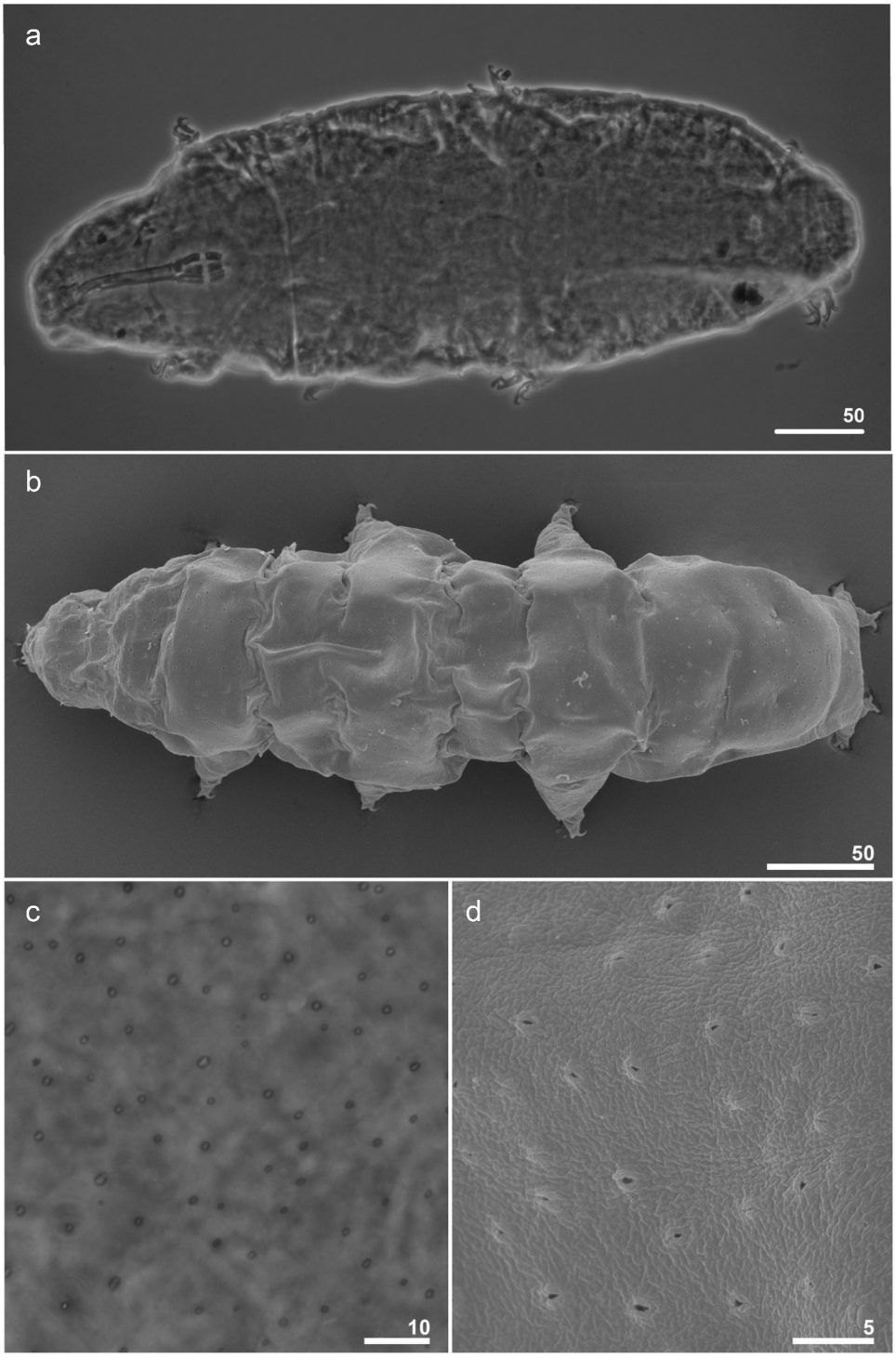

Figure 2. *Diaforobiotus quetzalcoatli* sp. nov., habitus: (a) dorso-lateral projection of the entire animal (holotype, Phase Contrast Microscopy (PCM)); (b) dorsal view of the entire animal Scanning Electron Microscopy (SEM). (**c–d)** aspect of cuticle showing the cuticular pores (PCM and SEM, respectively). Scale bars in micrometres (µm).

Type locality

Mount Tlaloc (Figure 1), State of Mexico, Mexico. In the moss *Grimmia elongata* (Kaulf.) Brid. 1816 on rock; GenBank code: PV077283) from alpine grassland; altitude 4037 m a.s.l. 19°24′46.1′′N, 98°43′05.2′′W.

Table 4. Measurements (in µm) and *pt* values of morphological structures of the holotype and paratypes of *Diaforobiotus quetzalcoatli* sp. nov. *N* = number of specimens/structures measured; range = the smallest and the largest structure among all measured specimens; SD = standard deviation.

		RANGE		MEAN		SD		Holotype	
CHARACTER	N	µm	*pt*	µm	*pt*	µm	*pt*	µm	*pt*
Body length	23	220–776	*534–1312*	545	*927*	152	*181*	659	*1022*
Diameter of pores in anterior region	8	0.4–3.1							
Diameter of pores in dorsal	6	0.3–2.2							
Diameter of pores ventral	5	1.3–2.0							
Diameter of pores in legs	5	1.3–2.4							
Buccopharyngeal tube									
Buccal tube length	23	40.1–69.6	–	57.2	–	8.1	–	64.5	–
Stylet support insertion point	21	29.9–55.8	*71.0–80.1*	43.0	*75.9*	6.8	*2.1*	49.9	*77.4*
Buccal tube external width	22	4.6–9.8	*9.8–15.9*	7.6	*13.4*	1.5	*1.6*	9.4	*14.6*
Buccal tube internal width	22	3.0–7.7	*6.6–13.3*	5.4	*9.6*	1.2	*1.9*	4.4	*6.8*
Ventral lamina length	13	23.6–49.5	*54.2–75.1*	34.5	*59.8*	6.6	*5.6*	37.5	*58.1*
Placoid lengths									
Macroplacoid 1	20	7.8–19.1	*16.8–30.7*	13.7	*24.1*	3.2	*4.1*	13.8	*21.4*
Macroplacoid 2	20	5.6–12.0	*13.8–18.0*	9.0	*15.8*	1.9	*1.5*	11.6	*18.0*
Macroplacoid row	20	14.4–33.7	*35.8–52.8*	25.2	*44.3*	5.3	*5.1*	27.9	*43.3*
Claw I heights									
External base	5	5.4–11.6	*9.7–18.0*	8.6	*14.3*	2.9	*3.7*	11.6	*18.0*
External primary branch	5	6.2–7.3	*11.2–12.5*	6.9	*11.7*	0.5	*0.6*	7.3	*11.3*
External secondary branch	5	3.6–4.8	*6.5–8.3*	4.4	*7.4*	0.5	*0.6*	4.8	*7.4*
External base/primary branch (cct)	4	78.9–158.4	–	113.8	–	33.1	–	?	–
Internal base	6	4.4–13.3	*11.0–20.2*	8.7	*14.7*	3.6	*4.1*	11.2	*17.4*
Internal primary branch	6	6.6–7.3	*10.5–16.4*	7.1	*12.5*	0.3	*2.1*	7.3	*11.3*
Internal secondary branch	6	4.1–5.6	*6.3–11.6*	4.8	*8.5*	0.6	*2.2*	4.4	*6.8*
Internal base/primary branch (cct)	5	66.9–191.5	–	116.8	–	52.9	–	?	–
Claw II heights									
External base	4	5.1–10.8	*9.7–16.7*	8.2	*14.5*	3.1	*3.3*	10.8	*16.7*
External primary branch	4	4.5–8.6	*10.8–13.3*	6.8	*12.2*	2.1	*1.4*	8.6	*13.3*
External secondary branch	4	3.6–4.9	*6.9–10.4*	4.4	*8.1*	0.6	*1.5*	4.9	*7.6*
External base/primary branch (cct)	4	89.1–132.3	–	118.1	–	19.6	–	125.6	–
Internal base	4	9.2–13.4	*15.0–20.8*	11.8	*18.4*	2.0	*2.9*	13.4	*20.8*
Internal primary branch	4	6.6–8.6	*10.2–13.1*	7.4	*11.6*	1.0	*1.6*	6.6	*10.2*
Internal secondary branch	4	4.6–5.9	*7.1–9.0*	5.1	*8.0*	0.7	*1.0*	4.6	*7.1*
Internal base/primary branch (cct)	4	116.7–203.9	–	163.5	–	46.5	–	203.0	–
Claw III heights									
External base	5	5.5–10.6	*9.6–18.9*	7.2	*13.2*	2.0	*3.9*	6.2	*9.6*
External primary branch	5	5.0–7.0	*7.8–12.3*	5.8	*10.7*	0.9	*1.8*	5.0	*7.8*
External secondary branch	4	3.4–5.2	*6.7–8.6*	4.2	*7.9*	0.8	*0.8*	?	?
External base/primary branch (cct)	5	87.3–179.5	–	123.7	–	34.8	–	124.0	–
Internal base	3	7.7–9.9	*11.9–17.6*	8.4	*14.1*	1.2	*3.1*	7.7	*11.9*
Internal primary branch	3	6.3–11.9	*11.3–19.7*	10.0	*16.5*	3.2	*4.6*	11.9	*18.4*
Internal secondary branch	3	5.2–8.2	*9.2–13.6*	7.2	*11.8*	1.7	*2.3*	8.2	*12.7*
Internal base/primary branch (cct)	3	64.6–156.3	–	95.2	–	52.9	–	64.7	–
Claw IV heights									
Anterior base	6	6.4–14.1	*12.2–25.8*	11.4	*19.6*	3.8	*4.8*	13.8	*21.4*
Anterior primary branch	6	6.1–12.9	*11.6–19.6*	9.0	*15.7*	2.5	*2.8*	8.9	*13.8*
Anterior secondary branch	6	4.5–8.7	*8.9–13.2*	6.1	*10.7*	1.6	*1.5*	6.1	*9.5*
Anterior base/primary branch (cct)	6	95.9–155.1	–	125.1	–	25.7	–	155.1	–
Posterior base	7	7.3–15.8	*15.4–24.0*	11.8	*20.4*	3.2	*3.1*	12.8	*19.8*
Posterior primary branch	7	4.8–10.7	*9.2–17.8*	8.4	*14.5*	2.3	*2.9*	9.5	*14.7*
Posterior secondary branch	7	4.0–7.9	*7.6–12.0*	5.8	*10.1*	1.6	*1.8*	6.3	*9.8*
Posterior base/primary branch (cct)	7	120.6–167.7	–	142.3	–	14.9	–	134.7	–

Description of the new species

Animals (measurements and statistics in Table 4). The body is light green in live specimens and transparent after mounting in Hoyer and PVA media. Eyes are present in all specimens mounted in slides. The body has a smooth cuticle (Figure 2(a, b)). Circular and oval pores are present with irregular distribution all over the body (visible in live animals) (Figures 2(c, d) and 3(b)). Pores around the mouth opening are present. Rigid buccal tube with a slight curvature in the anterior portion. Ventral lamina present (Figure 4(a)). In the buccal armature, three bands of teeth are present (Figure 5(a–d)): the first two bands are formed by small and numerous teeth, that are imperceptible in PCM but visible in SEM (Figure 5); the second band of teeth is larger than the third band, which is visible in PCM and SEM. Teeth of the first band 0.07–0.13 µm in height, the teeth of the second band 0.32–0.44 µm in height; details in Table 5. The third band presents, both ventrally and dorsally, two large

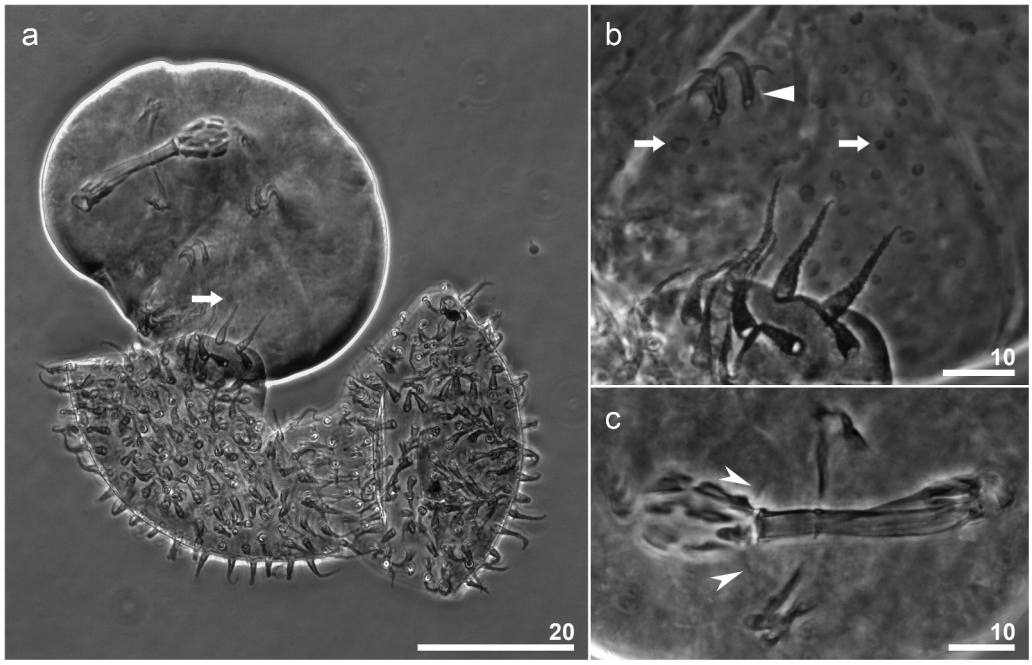

Figure 3. *Diaforobiotus quetzalcoatli* sp. nov., juvenile hatching from the egg: (a) general view of the hatching animal: (b) a closer view of the egg processes in the first plane, and the cuticle of the animal in the second plane. (**c)** buccopharyngeal apparatus. Arrows indicate the cuticular pores; arrowheads indicate the claws II; indented arrowheads indicate the dorsal spikes. Scale bars in micrometres (μm).

and pointed teeth (0.93 μm in height), as well as a rounded median tooth (in PCM). The teeth of the third band and the medial tooth are arranged in a triangular configuration (Figure 5(c, d)). The medial tooth is between 0.6 and 1.2 μm in height and between 0.7 and 1.4 μm in width (tooth measurements are detailed in Table 5). The distance between the two anterior teeth of the third band is 3.0–4.9 μm, while the distance between the two anterior teeth and the medial tooth of the third band is 2.8–4.0 μm. The stylet support insertion point is located close to the pharyngeal bulb. Inside the pharyngeal bulb a triangular apophysis and a row of two macroplacoids (with sequence 1 > 2) present (Figure 4(b)). The macroplacoids are rod shaped, with the first one showing a slight medial constriction and the second an evident subterminal constriction (Figure 4(b)). The microplacoid and septulum are absent. In most specimens two cuticular spikes were observed between the apophysis and the end of the buccal tube (Figure 4(a)). The claws are of the Richtersiusidae type with accessory points on primary branches (Figure 6(a–d)). Cuticular bars under the claws are present (Figure 6 (a)). The lunules on claws I–III are smooth, small, and shaped like amorphous trapezoids (Figure 6(a, c)), while those on claws IV are indented with small teeth (Figure 6(b, d)). Granulation on all legs is absent. Pulvinus in legs I–III are present (Figure 6(e, f)). The lines of musculature can be seen on legs IV (Figure 6(b)).

Eggs (measurements and statistics in Table 6). Egg spherical (Figures 7 and 8). In PCM, the surface between the processes presents faint dark dots, evenly distributed (Figures 7(c, d)). With SEM, the surface is smooth without pores or reticulation (Figure 8(b)). The processes are slender and conical with apices filamentous (projected at the top) (Figures 7(b), 8(a–d)). The surface of the process is covered with granulation from the proximal to distal sections (Figures 7(b, c) and 8(c, d)).

Reproduction

The new species is dioecious; the males have testes, and the females have ovaries. No evidence of sperm allowed us to compare their shape.

Type material repositories

The holotype (Slide TLPR 37) and 15 paratypes (Slides TLPR 1–33) are deposited in the Tardigrada Collection at the Colección Nacional de Insectos (CNIN) at the Institute of Biology, Instituto de Biología-Universidad

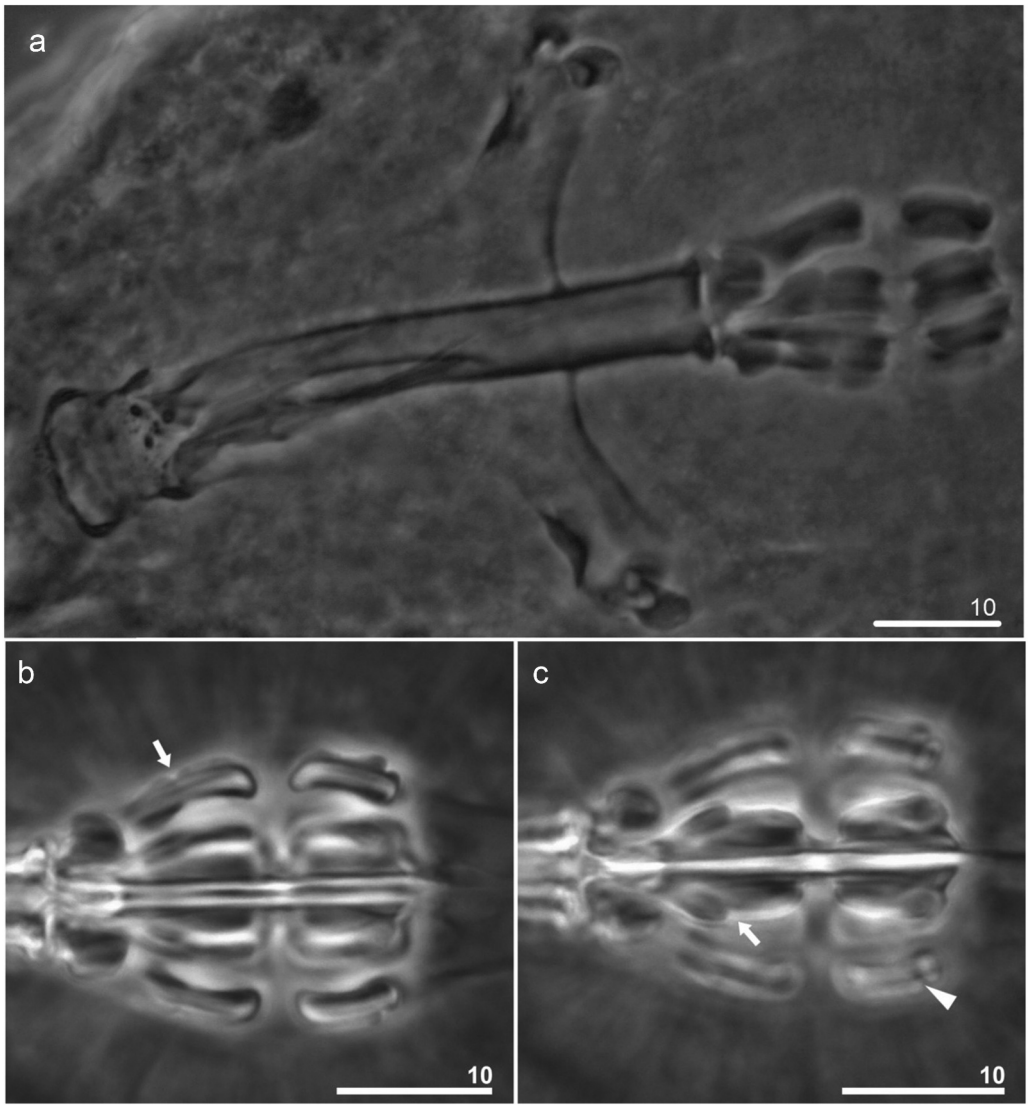

Figure 4. *Diaforobiotus quetzalcoatli* sp. nov., buccopharyngeal apparatus (dorso–ventral projection in PCM): (a)general view (holotype); (**b–c)** dorsal and ventral placoids, respectively (paratype); arrows indicate the central constriction in the first macroplacoid; arrowhead indicates subterminal constriction in the second macroplacoid; empty arrowheads indicate the dorsal spikes. Scale bars in micrometres (μm).

Nacional Autónoma de México (IBUNAM). Two paratypes (Slides TLPR27 and TLPR71) are deposited in the Bertolani collection at the University of Modena and Reggio Emilia, Italy (UNIMORE).

Etymology. The species is named after the god Quetzalcoatl, brother of the god Tlaloc (the name given to the mountain where the study site is located) in Aztec history. Quetzalcoatl is a cultural hero, often depicted as a feathered serpent ("serpiente emplumada" in Spanish), or one adorned with beautiful feathers. In Mesoamerican culture, depictions of this god often feature shades of green, similar to those observed in *Diaforobiotus quetzalcoatli* sp. nov. The species name is constructed as a possessive formed directly from the personal name "Quetzalcoatl". This name is masculine and singular; thus, we use the ending "**-i"**. So, the species is named in honour of the god Quetzalcoatl (following the International Code of Zoological Nomenclature, 1999).

Moss identification

Morphological and molecular data were available to identify the moss from which *D. quetzalcoatli* sp. nov. was extracted, as *Grimmia elongata* (Kaulf.) Brid. 1816. The presence of sporophytes in the moss indicates a

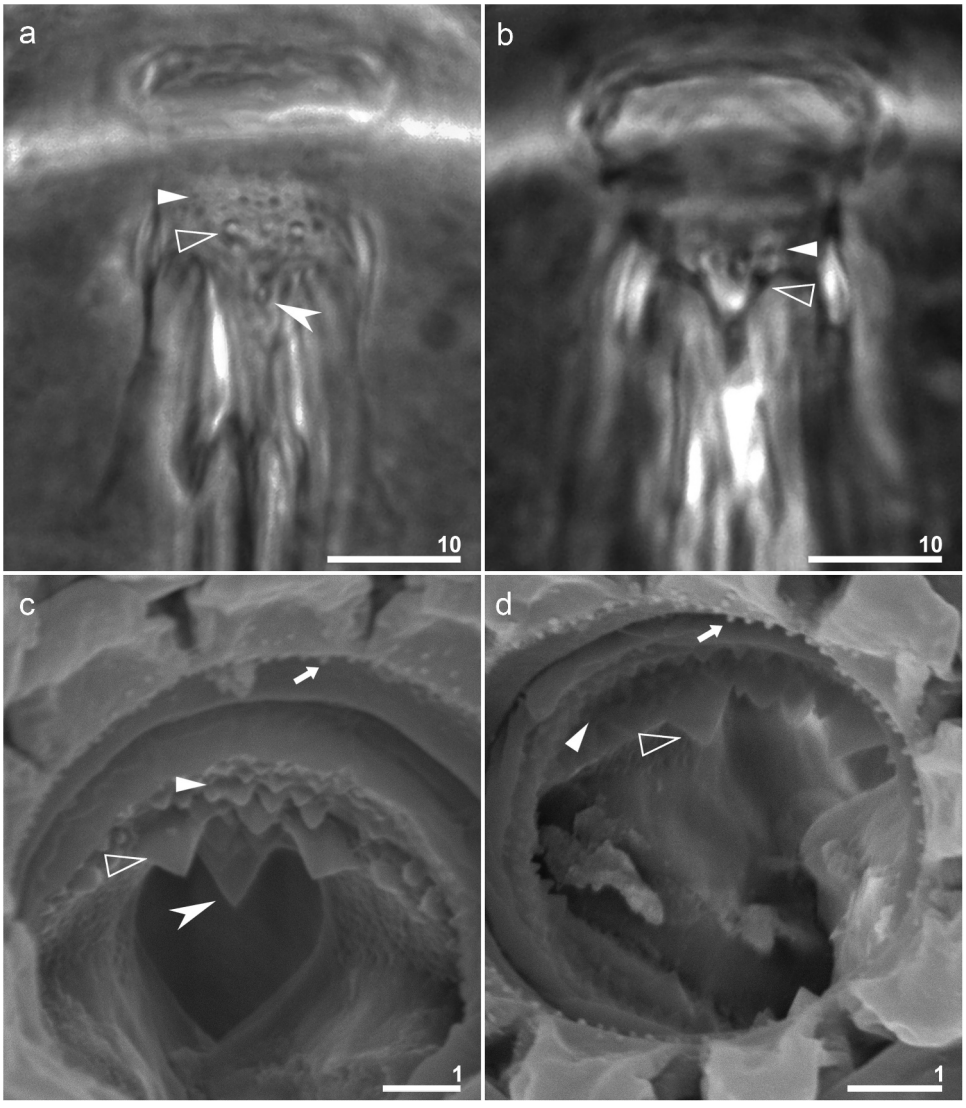

Figure 5. *Diaforobiotus quetzalcoatli* sp. nov., oral cavity armature: (**a**–b) dorsal and ventral views, respectively (paratype); (**c–d)** dorsal and ventral views, respectively (SEM); the arrow indicates teeth of the first band; flat arrowheads indicate teeth of the second band; empty arrowheads indicate teeth of the third band; indented arrowheads indicate the medial tooth in dorsal. Scale bars are in micrometres (µm).

Table 5. Measurements of distance between teeth in *Diaforobiotus quetzalcoatli* sp. nov. *N* = number of structures measured; range = the smallest and the largest structure among all measured specimens; SD = standard deviation.

		RANGE		MEAN		SD	
CHARACTER	N	µm	*pt*	µm	*pt*	µm	*pt*
Heights of teeth in the first and second bands							
Teeth of the first band (height)	6	0.07–0.13	*0.33–0.33*	0.11	*0.3*	0.0	?
Teeth of the first band (width)	6	0.09–0.23	*0.32–0.32*	0.13	*0.3*	0.0	?
Teeth of the second band (height)	4	0.32–0.44	*0.80–0.80*	0.40	*0.8*	0.1	?
Teeth of the second band (width)	4	0.31–0.54	*0.77–0.77*	0.45	*0.8*	0.1	?
Third band teeth distance							
Between the teeth of the third band	6	2.97–4.85	*4.82–7.81*	3.86	*6.5*	0.7	*1.1*
Between the tooth of the third band and medial	6	2.75–3.96	*4.80–5.97*	3.28	*5.5*	0.4	*0.4*
Medial tooth height (SEM)	4	0.63–1.16	?	0.93	?	0.2	?
Medial tooth width (SEM)	4	0.69–1.37	?	0.99	?	0.3	?

Table 6. Measurements of morphological structures of the eggs of *Diaforobiotus quetzalcoatli* sp. nov. mounted in PVA medium. *N* = number of eggs/structures measured; range = the smallest and the largest structure among all measured specimens; SD = standard deviation.

CHARACTER	N	RANGE (µm)	MEAN	SD
Egg bare diameter	3	123–151	139	15
Egg full diameter	3	165–184	176.1	10
Process height	9	13.8–19.9	16.9	2.3
Process base width	9	2.3–3.3	2.8	0.3
Process base/height ratio	9	14%–22%	17%	3%
Inter-process distance	9	5.2–12.9	8	2.6
Number of processes on the egg circumference	3	30–36	32.3	3.2

mature specimen with the capacity to host numerous specimens and eggs of *D. quetzalcoatli* sp. nov. and other species of tardigrades in the microhabitat.

The partial RuBisCo gene from *Grimmia elongata* (Kaulf.) Brid. 1816 was represented by one haplotype (GenBank accession code): rbcL: PV077283.

Phylogenetic position and genetic delimitation of the new species

Phylogenetic reconstructions using BI and ML methods produced trees with similar topologies and mostly well-supported nodes, although the ML tree exhibited the lowest support values (refer to SM.04 and Figure 9). In our analysis, we recovered two monophyletic clades, corresponding to the genera *Diaforobiotus* and *Richterisus*. Consistent with Stec and Morek (2022), the *Richtersius* clade demonstrates a similar topology, with *R. coronifer* from Norway and *R. ziemowiti* from Nepal forming a sister pair to the other species within the genus (see Figure 9). Within *Diaforobiotus*, *D. hyperonyx* forms the sister lineage to a larger clade that includes all congeners. Within the remaining *Diaforobiotus*, the most basal split separates the (*D. islandicus*, *D. svalbardicus*) clade from a subclade (*D.* sp. *ID.517* + *D. occidentalis*, *D. quetzalcoatli*). The newly described species forms a strongly supported monophyletic group, including five sequences (sp. nov. 1, 5, 6, 7, and 17) of *D. quetzalcoatli* sp. nov. It is sister to a clade containing *D. occidentalis* (samples S2011 Dia.V01 and Dia.V02).

Regarding the COI dataset, sequences from the Mexican population exhibited low levels of sequence divergence, with uncorrected p-distance values ranging from 0.1% to 4.0%. In contrast, genetic distances between the Mexican sequences and those from other congeneric populations were substantially higher, ranging from 15.8% to 21.1%. Species delimitation analyses performed using both the PTP model and the ASAP method consistently grouped Mexican sequences together, forming a distinct lineage (Figure 10). The best partition generated by ASAP (ASAP score = 1.00; threshold p-distance = 8.99%) identified six groups of sequences, corresponding to six putative species: *Diaforobiotus quetzalcoatli* sp. nov. (Mexico), *D. hyperonyx* (Italy), *D. occidentalis* (Canada), *D. islandicus* (Iceland), *D. svalbardicus* (Norway), and an unidentified *Diaforobiotus* species from Indonesia (Figure 10). In the haplotype network analysis, five out of six Mexican sequences clustered closely together, while one sequence appeared slightly more divergent, exhibiting p-distance values between 2.3% and 4.0%, relative to the others from the same population (Figure 10).

For the ITS-2 dataset, species delimitation using ASAP identified three groups of sequences, corresponding to three putative species: *Diaforobiotus quetzalcoatli* sp. nov. (Mexico); *D. hyperonyx* (Italy); and a group comprising *D. islandicus*, *D. svalbardicus*, and an unidentified *Diaforobiotus* species from Indonesia (Figure 10). Although the resolution of ITS-2 was lower compared to COI, Mexican sequences consistently clustered together and were separated from other congeneric taxa. Genetic divergence among individuals from the Mexican population was very low, with p-distance values ranging from 0.0% to 0.23%. Haplotype network analysis based on ITS-2 further supported these results, grouping the Mexican sequences into a single distinct cluster, consistent with the pattern observed for the COI dataset. Overall, while the ITS-2 marker revealed slightly lower genetic variability and recovered fewer putative species than COI, the two markers provided congruent evidence for the genetic distinctiveness and internal cohesion of the Mexican population.

Genotypic differential diagnosis

The genetic divergence between the sequences analysed in the genus *Diaforobiotus* shows a range between molecular markers. The ranges of uncorrected genetic p-distances (shown in the Supplementary materials,

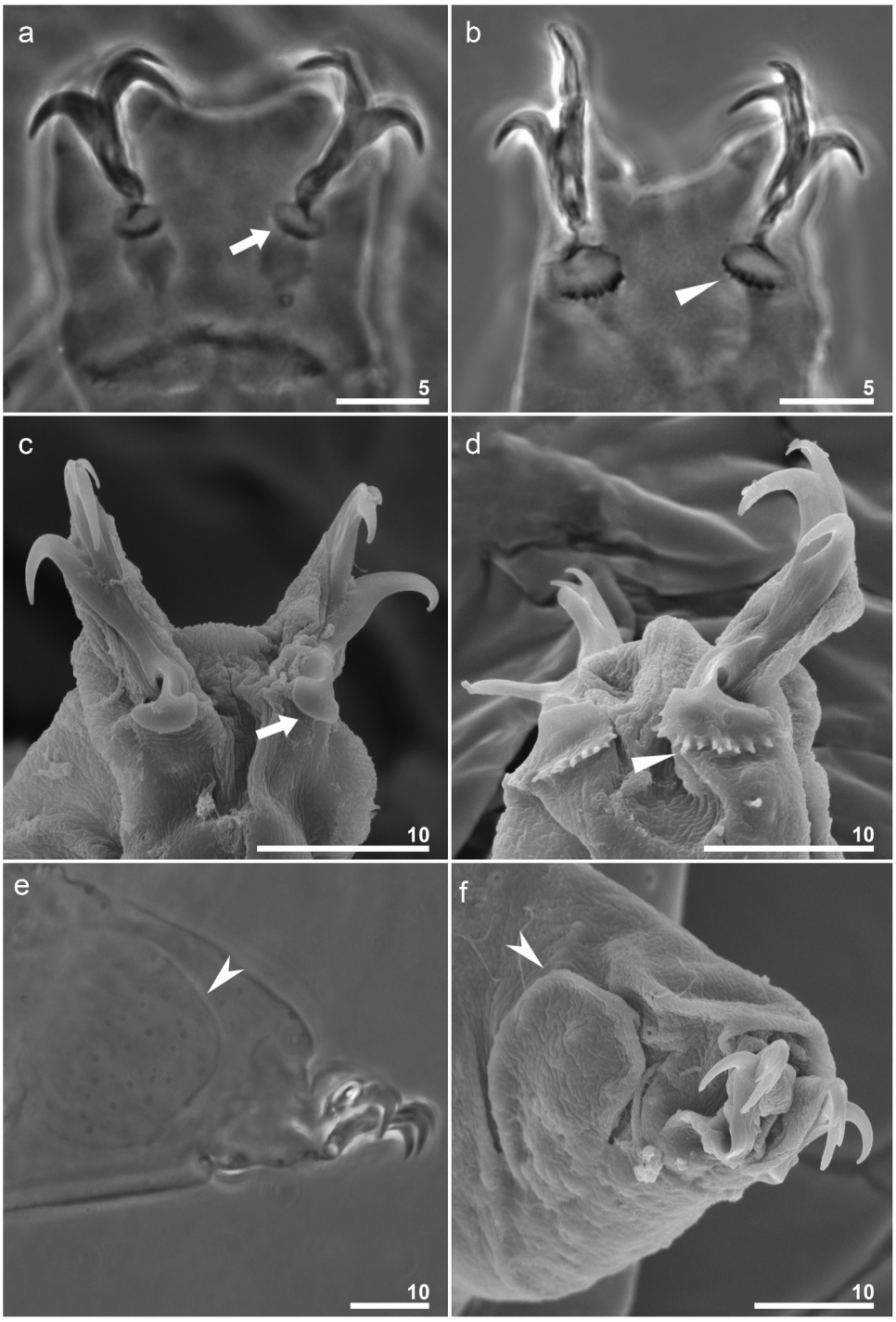

Figure 6. *Diaforobiotus quetzalcoatli* sp. nov., claws in PCM and SEM: (**a–**b) claws II and IV, respectively (PCM). (**c–d)** claws II and IV, respectively, seen in SEM. (**e–f)** claws III seen in PCM and SEM respectively (paratype); arrows indicate the smooth lunules under the claws II; arrowheads indicate the indented lunules under the claws IV; indented arrowheads indicate the pulvinus on the internal surface of the leg III. Scale bars in micrometres (μm).

SM.02), from the most to the least conservative between the new species and other species of the genus *Diaforobiotus* for which sequences are available from GenBank, are as follows:

- **COI**: 16.0–22.0%, with the most similar species being *D. occidentalis* MV2022 Dia2 from Canada (OQ029492), and the least similar species being *D. hyperonyx* IT.341 from Italy (OM151288).

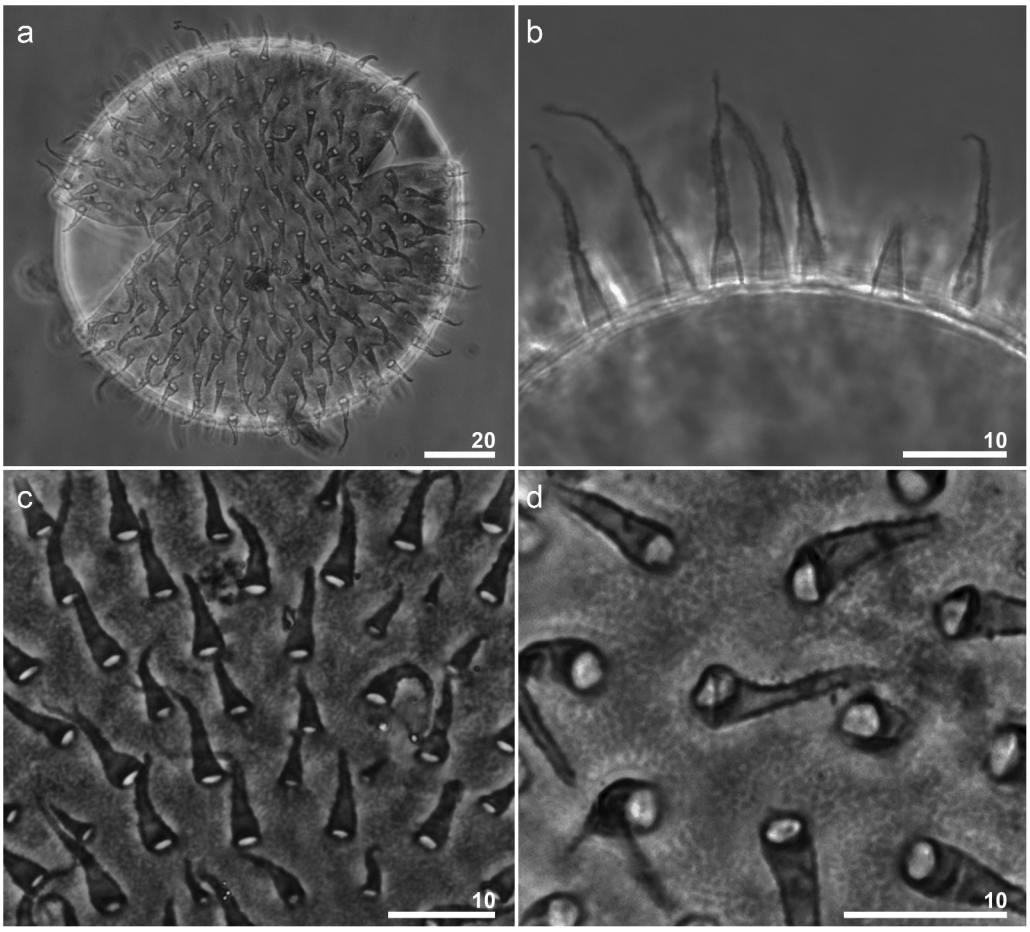

Figure 7. *Diaforobiotus quetzalcoatli* sp. nov., eggs seen in PCM: (a) the surface seen in PCM; (b) focus on egg processes in the circumference seen in PCM; (**c–d)** focus on egg surface between processes seen in PCM. Scale bars in micrometres (μm).

- **ITS-2**: 12.0–20.0%, with the most similar species being *D. islandicus* IS. 042 from Iceland (MT812597), and the least similar species being *D. hyperonyx* IT.344 from Italy (OM179867).
- **18S**: 0.30–1.62%, with the most similar species being *D. occidentalis* Haida Gwaii 1 from Canada (OQ029310), and the least similar species being *D. hyperonyx* IT.344 from Italy (OM179867).
- **28S**: 1.25–49.75%, with the most similar species being *D. islandicus* IS. 042 from Iceland (MT812597), and the least similar species being *D. islandicus* TarCPH23 from Spain (MH079486).

Phylogenetic analyses based on Bayesian and ML methods confirm that *D. quetzalcoatli* sp. nov. forms a well-differentiated monophyletic clade, sister to *D. occidentalis* from Canada, with very low support values (Bayesian posterior probabilities > 0.90 and bootstrap support > 50), and separated from another clade comprising European species. The haplotype network further highlights *D. quetzalcoatli* sp. nov.'s unique genetic structure, distinct from European species, revealing six putative species with COI and three with ITS-2, which demonstrates a consistent and differentiated internal variability among its congeners. Additionally, genetic divergence percentages (COI, ITS-2, 18S rRNA, and 28S rRNA) exceed the usual speciation threshold in the genus, supporting the validity of *D. quetzalcoatli* sp. nov. as a new species and providing a basis for its morphological description and delimitation.

The three nuclear markers and one mitochondrial marker were represented (GenBank accession codes SM.03): 18S rRNA: PV018904-PV018908; 28S rRNA: PV018909-PV018915; ITS-2: PV018916-PV018923 (H1) and COI with two haplotypes: PQ506034-PQ506035 and PV017055-PV017058) from *D. quetzalcoatli* sp. nov.

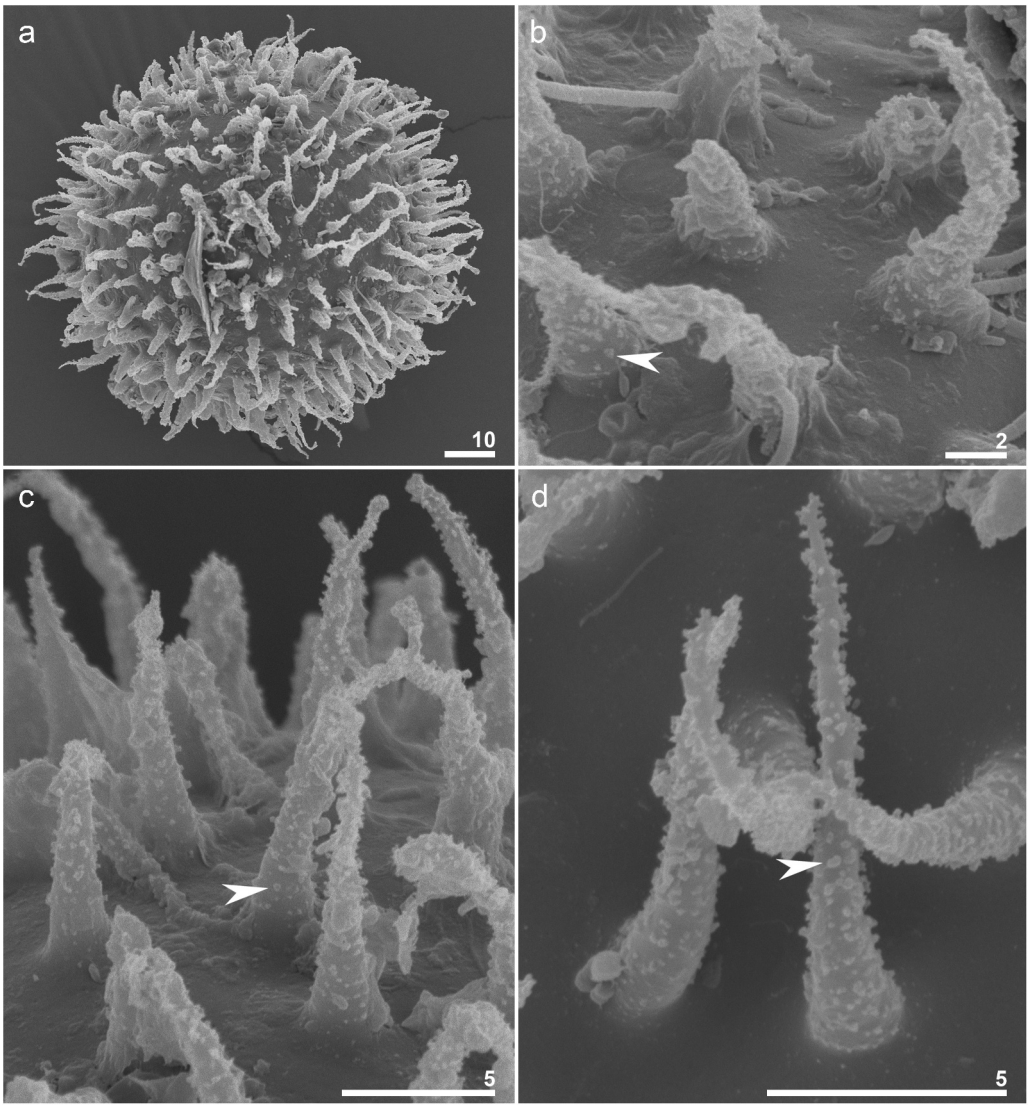

Figure 8. *Diaforobiotus quetzalcoatli* sp. nov., eggs seen in SEM: (a) general view of the entire egg; (**b–d)** details of the egg surface and egg processes. Indented arrowheads indicate the granulation on the process surface. Scale bars are in micrometres (µm).

Morphological differential diagnosis

Currently, there are five species within *Diaforobiotus*: *D. caelicola* (Kathman 1990), *D. hyperonyx*, *D. islandicus*, *D. occidentalis* and *D. svalbardicus* (Stec 2023; Degma & Guidetti 2024, Massa et al. 2024). *Diaforobiotus quetzalcoatli* sp. nov. stands out from other species within the genus due to its unique combination of traits, including smooth eggs, light green pigmentation, and an elongated egg process that differs from those of *D. svalbardicus*, *D. islandicus*, and *D. hyperonyx*. Furthermore, it presents distinctive morphometric measurements across various anatomical structures, further supporting its differentiation from related species. Moreover, *D. quetzalcoatli* sp. nov. differs specifically from:

- *D. caelicola* (Kathman, 1990), known only from its type locality in Colorado, USA (Kathman 1990), by a slightly larger body length (up to 668 µm in *D. caelicola* vs up to 776 µm in *D. quetzalcoatli* sp. nov.). By shorter primary branches on leg II (17.5 µm in *D. caelicola* [holotype] vs 4.5–8.6 µm in external primary branch and 6.6–8.6 µm in internal primary branch in *D. quetzalcoatli* sp. nov.). By shorter primary branches on claws IV (32.5 µm in *D. caelicola* [holotype] vs 6.1–12.9 µm in anterior primary branch and 4.8–10.7 µm in posterior primary branch in *D. quetzalcoatli* sp. nov.). By a shorter egg process height (up to 34 µm in *D. caelicola* vs up to 19.9 µm in *D. quetzalcoatli* ***sp. nov***.). By the morphology of apex processes (apices divided into multi-tipped points in *D. caelicola* vs filamentous without division at the apices in *D. quetzalcoatli* **sp. nov**.).

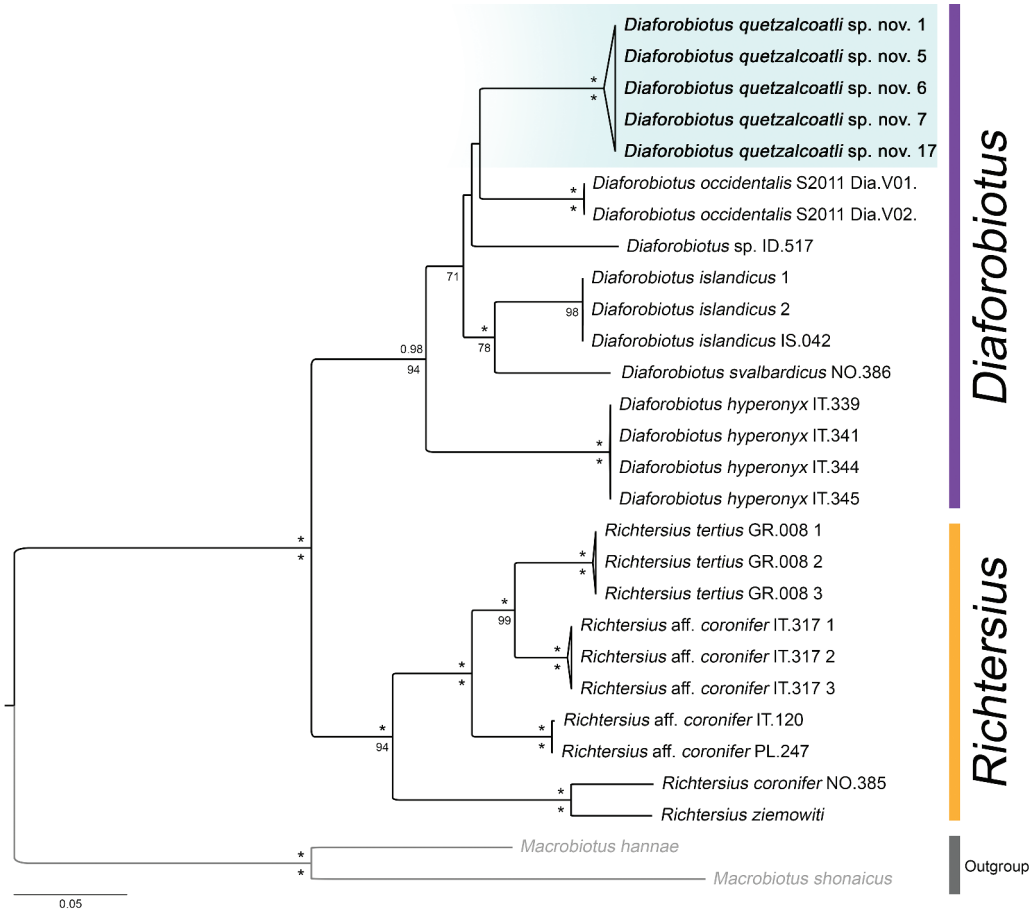

Figure 9. Phylogenetic tree constructed from concatenated sequences of the family Richtersiusidae (18S rRNA + 28S rRNA + ITS-2 + COI). Numbers above branches indicate Bayesian posterior probability values (≥0.90), while numbers below branches indicate bootstrap support values (≥50), and asterisks indicate maximal support. The outgroup is indicated in grey font. The new species is in bold font. The scale bar represents substitutions per position.

- *D. hyperonyx* (Maucci, 1982), known only from its type locality in Italy (Maucci 1982; Stec & Morek 2022), by the presence of three teeth in the dorsal portion of the third band of the oral armature, by a larger buccal tube internal width (*pt 4.6–6.5* in *D. hyperonyx* vs *pt 6.6–13.3* in *D. quetzalcoatli* **sp. nov**.). By the claw common tract longer than half of the entire claw height, by a smaller external primary branch in claw I (*pt 41.6–63.3* in *D. hyperonyx* vs *pt 11.2–12.5* in *D. quetzalcoatli* **sp. nov**.). By a smaller external secondary branch in claw I (*pt 21.0–31.0* in *D. hyperonyx* vs *pt 6.5–8.3* in *D. quetzalcoatli* **sp. nov**.). By a smaller anterior primary branch in claw IV (*pt 62.8–97.1* in *D. hyperonyx* vs *pt 11.6–19.6* in *D. quetzalcoatli* sp. nov.). By a shorter distance between the third band of teeth and the medial tooth (4.52 µm in *D. hyperonyx* vs 3.0–4.0 µm in *D. quetzalcoatli* **sp. nov**.). By a greater length of the medial tooth (0.923 µm in *D. hyperonyx* vs 0.6–1.2 µm in *D. quetzalcoatli* **sp. nov**.). By the larger height of the egg processes (9.4–11.9 µm in *D. hyperonyx* vs 13.8–19.9 µm in *D. quetzalcoatli* **sp. nov**.).
- *D. islandicus* (Richters, 1904), known from its type locality in Iceland (Richters 1904; Stec 2023) and reported in North America (Kaczmarek et al. 2016; Moreno-Talamantes & León-Espinosa 2019), by a longer distance between the third band of teeth and the medial tooth (3.18 µm in *D. islandicus* vs 4.0 µm in *D. quetzalcoatli* **sp. nov**.). By a shorter external primary branch in claw I (*pt 24.7–30.2* in *D. islandicus* vs *pt 11.2–12.5* in *D. quetzalcoatli* **sp. nov**.). By a shorter anterior primary branch in claw IV (*pt 28.1–37.7* in *D. islandicus* vs *pt 11.6–19.6* in *D. quetzalcoatli* **sp. nov**.). By the absence of pores in eggs (vs pores present as a ring in the base of the processes in *D. islandicus*). By a larger egg diameter (88.5–101.4 µm in *D. islandicus* vs 123–151 µm in *D. quetzalcoatli* **sp. nov**.). By a larger height in the egg processes (5.9–11.2 µm in *D. islandicus* vs 13.8–19.9 µm in *D. quetzalcoatli* **sp. nov**.).

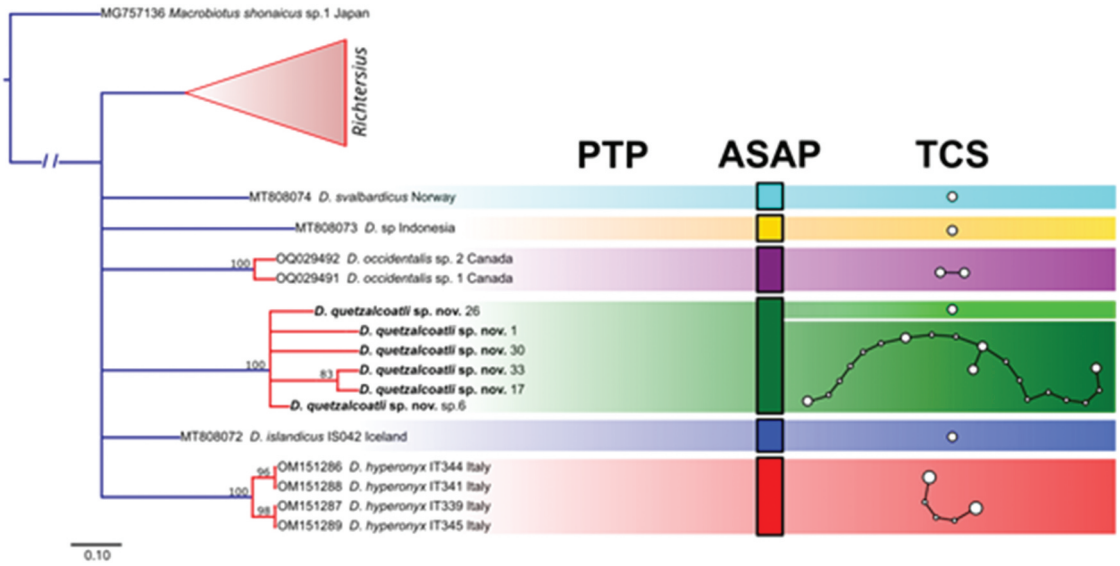

Figure 10. Species delimitation based on 648 bp of the COI gene of *Diaforobiotus* and *Richtersius* species. The tree resulting from maximum likelihood analysis is shown on the left; values above branches represent the bootstrap values. PTP represents the results of the Poisson tree process analysis, and it is shown in different colours of branches: putative species are indicated using transitions from blue to red branches. The ASAP analysis (centre) shows groups of specimens with the lowest ASAP score (1.00) as indicated with a rectangular shape. The haplotype network analysis is shown on the right; the circles show the haplotypes, and their size indicates the haplotype frequency, while the dots show putative haplotypes.

- *D. occidentalis* (Murray 1910), known from its type locality in Victoria, British Columbia, Canada (Murray 1910), and reported in Costa Rica (Kaczmarek et al. 2014a), Argentina, Brazil, Peru (Kaczmarek et al. 2016), Greenland, and the USA (Kaczmarek et al. 2016), by a longer distance between the third band of teeth and the medial tooth (3.00 µm in *D. occidentalis* vs 4.0 µm in *D. quetzalcoatli* sp. nov.). By a smaller external primary branch in claw I (*pt 23.5–29.0* in *D. occidentalis* vs *pt 11.2–12.5* in *D. quetzalcoatli* sp. nov.). By a shorter anterior primary branch in claw IV (*pt 29.9–36.4* in *D. occidentalis* vs *pt 11.6–19.6* in *D. quetzalcoatli* sp. nov.). By the absence of microplacoid (present in *D. occidentalis*). By a greater egg diameter (83.2–90.7 µm in *D. occidentalis* vs 123–151 µm in *D. quetzalcoatli* sp. nov.).

Diaforobiotus svalbardicus Stec 2023, known only from its type locality in Svalbard, Norway (Stec 2023), by a smaller distance between the third band and the medial tooth (5.17 µm in *D. svalbardicus* vs 4.0 µm in *D. quetzalcoatli* sp. nov.). By a smaller medial tooth (1.16 µm in *D. svalbardicus* vs 0.6–1.2 µm in *D. quetzalcoatli* sp. nov.). By a smaller external primary branch in claw I (*pt 31.2–34.2* in *D. svalbardicus* vs *pt 11.2–12.5* in *D. quetzalcoatli* sp. nov.). By a smaller anterior primary branch in claw IV (*pt 33.2–42.9* in *D. svalbardicus* vs *pt 11.6–19.6* in *D. quetzalcoatli* sp. nov.). By a large egg bare diameter (107.2–125.9 µm in *D. svalbardicus* vs 123–151 µm in *D. quetzalcoatli* sp. nov.). By a large process height (7.9–12.4 µm in *D. svalbardicus* vs 13.8–19.9 µm in *D. quetzalcoatli* sp. nov.).

Dichotomous key for the genus Diaforobiotus

(modified from Stec 2023 and from; Massa et al. 2024).

The dichotomous key for the genus *Diaforobiotus* comprises five valid species, along with .... *D. quetzalcoatli* sp. nov.

1. - Teeth present on lunulae of legs I–III (e.g. Figure 6(b, d))..... ..... (2)
- Teeth absent on lunulae of legs I–III (Figure 6(a, c))..... (3)

2. - The claw common tract is longer than half of the entire claw height, egg surface between processes with evenly distributed dark dots (visible in PCM; e.g. Figure 7(d))..... ..... *Diaforobiotus islandicus* (Richters 1904)
- The claw common track constitutes one-third of the entire claw length, egg surface between processes without dark dots (visible in PCM)..... ..... *Diaforobiotus caelicola* (Kathman 1990)

3. - The claw common tract shorter than half of the entire claw length, the dorsal portion of the third

band of teeth in the buccal armature—where the transversal ridge is generally present,—comprises only one tooth..... *Diaforobiotus hyperonyx* (Maucci 1982)
- The claw common tract is longer than half of the entire claw height, dorsal portion of the third band of teeth in the buccal armature—where the transversal ridge is generally present—comprises three teeth(4)

4. - Microplacoid present (even if small and not always clearly visible), chorion surface with irregularly distributed dark dots on the egg surface between processes (visible in PCM), egg process base/height ratio 23–50%..... *Diaforobiotus occidentalis* (Murray 1910)
- Microplacoid absent (Figure 4)..... (5)

5. - Egg surface between processes without dots (only very few, evenly distributed, minute and faintly light-refracting dots may be visible in PCM), egg process base/height ratio 56– 83%..... *Diaforobiotus svalbardicus* Stec 2023
- Dots on the egg surface between processes (visible in PCM, but not in SEM), egg process base/height ratio 14–22%..... *Diaforobiotus quetzalcoatli* sp. nov.

Discussion

Diaforobiotus is a relatively recent genus that currently comprises five species and two subspecies (Guidetti et al. 2016; Stec & Morek 2022; Stec 2023; Massa et al. 2024; this study). The presence of dented lunules on leg pair IV may represent a homoplastic trait, as similar structures occur in other tardigrade taxa. Among the known *Diaforobiotus* species, *D. svalbardicus* exhibits the largest tooth measurements, whereas *D. hyperonyx* has the smallest. The buccal armature emerges as a key morphological feature with potential applicability to other taxa; in this study, parameters such as tooth height, width, and spacing proved valuable for distinguishing the new species. These features remain consistent within species and may serve as reliable indicators for assessing both intra- and interspecific variability, provided specimens are correctly oriented and mounted in an appropriate medium.

The smooth surface on the egg, the smooth lunules on legs I–III, the green pigmentation, and the morphometric characteristics of *Diaforobiotus quetzalcoatli* sp. nov. were also important traits distinguishing this species. However, some species within the genus lack essential information required by modern standards for species descriptions or descriptions. Particularly, *D. caelicola* and *D. islandicus nicaraguensis* (Séméria 1985) should be re-collected from their type localities and re-examined to obtain morphometric data, molecular analyses, and high-resolution microscopy images, which would help clarify their phylogenetic relationships within the genus (Richters 1904; Murray 1910; Séméria 1985; Kathman 1990; Maucci 1982; Stec 2023; Massa 2024). The original description of *D. islandicus nicaraguensis* provides a valuable initial account; however, it is somewhat limited, as it lacks detailed morphometric data and photographic documentation, and includes only a single schematic illustration of the egg (Séméria 1985). Similarly, although *D. caelicola* was described with some morphometric data and schematic illustrations, further investigation is needed to clarify key morphological features, such as the distribution of buccal teeth and cuticular pores, as well as the surface structure of the egg (Kathman 1990). Molecular data is essential to evaluate the phylogenetic position of both species within *Diaforobiotus*.

The diagnosis of *D. occidentalis* was recently revised by Massa et al. (2024). However, the measurements of some structures and the morphological characters in the original description by Murray (1910) suggest that the species found by Massa et al. (2024) may be a distinct taxon. In the description and scheme of *D. occidentalis* by Murray (1910), the microplacoid (which he refers to as "comma") is absent, whereas Massa et al. (2024) identified this structure in the specimens they examined. Notably, Murray described and illustrated the presence of a microplacoid in other species, implying that it would have been improbable for him not to draw it. However, as noted by Massa et al. (2024), the small size of this structure might have resulted in its being overlooked by Murray at the time. Nevertheless, as the original type material has been lost (Massa et al. 2024), it is imperative to conduct a redescription and neotype designation for this species, which remains somewhat enigmatic. As evidenced by Massa et al. (2024), it could be useful to examine additional species to reassess their classification.

The phylogenetic analyses presented in this study are consistent with the topology of Stec and Morek (2022). Also, we included all available *Diaforobiotus* sequences from GenBank, along with the sequences of *D.*

quetzalcoatli sp. nov. Our phylogenetic analyses recovered two distinct clades, albeit with moderate support: the first clade comprises *D. occidentalis* and *D. quetzalcoatli* sp. nov., both distributed in the Americas; the second clade includes *D. svalbardicus* and *D. islandicus*, species from northern European islands. This topology aligns with the geographic distribution of the species and supports a division between American and European clades. *Diaforobiotus hyperonyx* represents the sister lineage to all other species within *Diaforobiotus*, a position that highlights its distinct evolutionary history. This observation, combined with the notable elongation of its claw primary branches, has led Stec and Morek (2022) to suggest that *D. hyperonyx* may warrant recognition as a separate genus (Tumanov 2005; Stec & Morek 2022). The placement of *D. quetzalcoatli* sp. nov. alongside *D. occidentalis* suggests a close relationship between these American taxa. However, to confirm distribution patterns and ecological traits, and to identify robust synapomorphies, broader sampling is needed—particularly the inclusion of additional *Diaforobiotus* taxa from both Mexico and South America (Guidetti et al. 2016).

Stec (2023) applied an integrative taxonomic approach to provide a detailed redescription of *D. islandicus* and to describe *D. svalbardicus*, thereby enhancing diagnostic resolution through the combination of morphological and molecular data. Despite this progress, several records of *D. islandicus* remain unverified and warrant re-examination under an integrative framework. Notably, specimens from Nuevo León, Mexico, reported by Moreno-Talamantes and León-Espinosa (2019), exhibit dentition in the lunules of legs I–IV, with the most pronounced structures on leg IV—features that correspond with those described by Stec (2023). However, the absence of eggs in the material examined by Moreno-Talamantes and León-Espinosa limits the reliability of the identification. Due to the lack of these key diagnostic structures, and without molecular confirmation, the assignment of these Mexican specimens to *D. islandicus* remains tentative. Therefore, additional sampling and comprehensive analyses—including scanning electron microscopy of the egg chorion and DNA sequencing—are essential to clarify the taxonomic status of these populations and to assess the southern extent of the species' distribution.

Recent advances have significantly improved the taxonomic resolution within *Diaforobiotus*. Massa et al. (2024) amended the diagnosis of *D. occidentalis* and provided the first molecular data for the species. Similarly, *D. hyperonyx* has been redescribed and genetically characterized by Stec and Morek (2022). In the present study, we contribute to this effort by offering an integrative description of *D. quetzalcoatli* sp. nov., incorporating both morphological and molecular data. With the addition of this new species, the number of *Diaforobiotus* species supported by combined morphological and genetic evidence now stands at five. Nevertheless, *D. caelicola*, despite having a relatively detailed morphological description, still lacks molecular data to support its phylogenetic placement (Stec & Morek 2022; Stec 2023; Massa et al. 2024).

It is important to emphasize that, although DNA sequencing has become a powerful tool for species identification, the limited availability of molecular data for a *Diaforobiotus* sequence, included in our phylogenetic tree (*D.* sp. *ID.517*), highlights the continued relevance of morphological characters. As Pilato (2024) observed, while molecular data are indispensable for detecting cryptic diversity, morphological traits remain fundamental for species diagnosis and classification, offering valuable taxonomic information that complements genetic analyses.

A comprehensive understanding of tardigrade diversity requires not only robust morphological and molecular data but also information on the microhabitats they occupy, which can offer critical ecological and taxonomic insights (Glime 2018). Despite their importance, detailed studies on microhabitat preferences remain scarce (Beasley 1972; Schuster & Toftner 1982), underscoring the need for more targeted ecological sampling in future research. The identification of *Grimmia elongata* as the microhabitat of *D. quetzalcoatli* sp. nov. provides valuable ecological context and contributes to our understanding of the species' specific locality. While previous studies have found no consistent or exclusive association between tardigrades and particular microhabitats (Zawierucha et al. 2017; Nelson et al. 2019), recognizing the precise substrate can reduce ambiguity in future surveys. Some tardigrade species may exhibit microhabitat specificity, and such information could be critical for detecting or rediscovering rare taxa. Therefore, incorporating molecular tools for the accurate identification of plant microhabitats, along with collaboration with bryophyte specialists, could enhance the ecological resolution of tardigrade studies and address a component of biodiversity that is often overlooked.

Distribution

The known distribution of *Diaforobiotus* species reveals a genus with broad ecological amplitude and discernible biogeographical patterns. Species inhabit a range of environments, from Arctic glacial regions such as Svalbard (*D. svalbardicus*, Stec 2023), temperate alpine zones in the Alps (*D. hyperonyx*, Maucci 1982; Stec & Morek 2022), and high-altitude grasslands in central Mexico (*D. quetzalcoatli* sp. nov.), to temperate forests in North America (*D. caelicola*, Kathman 1990; *D. occidentalis*; Murray 1910) and tropical zones in South America (*D. islandicus*, e.g. Meyer 2001; Johansson et al. 2013). This environmental diversity suggests both ecological plasticity and potential specialization within the genus. For instance, the restriction of *D. quetzalcoatli* sp. nov. to alpine grasslands may reflect specific ecological requirements, while the broad range of *D. islandicus* and *D. occidentalis*—recorded across the United States, Canada, Greenland, and Colombia—could indicate ecological generalism or unrecognized cryptic diversity (e.g. Séméria & Elin 1989; Jørgensen & Kristensen 1991; Meyer & Hinton 2012). Biogeographically, the grouping of *D. svalbardicus* and *D. islandicus* in northern European and North Atlantic regions, contrasted with the clustering of *D. occidentalis* and *D. quetzalcoatli* in the Americas, suggests a transcontinental divergence pattern possibly shaped by historical climatic events, such as glacial cycles (Nelson et al. 2019). While prior studies have shown no consistent correlation between tardigrade species and specific microhabitats (Zawierucha et al. 2017; Nelson et al. 2019), identifying the moss *Grimmia elongata* as the substrate for *D. quetzalcoatli* sp. nov. provides a more detailed ecological context. As emphasized by Glime (2018), microhabitat data are often overlooked but can be informative for understanding tardigrade distribution. Moreover, the scarcity of studies explicitly identifying host bryophytes (Beasley 1972; Schuster & Toftner 1982) underscores the importance of integrating molecular techniques alongside bryological expertise. Employing DNA barcoding or metabarcoding to accurately identify moss and liverwort species can complement traditional morphological identification, especially when dealing with cryptic or morphologically similar taxa. Additionally, high-resolution imaging methods such as SEM can provide detailed surface characterization of both tardigrades and their substrates. Together, these approaches would significantly enhance the ecological resolution of tardigrade research and clarify species–microhabitat associations that are often overlooked.

Conclusions

The genus *Diaforobiotus* comprises a diverse and widely distributed group within the family Richtersiusidae, with species inhabiting Arctic, temperate, and tropical regions across North America, South America, and Europe. Recent taxonomic and molecular studies, integrating morphological descriptions with genetic data, have significantly improved our understanding of the genus. Its broad geographical range, from glacial environments to tropical ecosystems, highlights its ecological adaptability. The presence of multiple species in Canada suggests that North America may serve as a centre of diversity for the group. However, the discovery of *D. quetzalcoatli* sp. nov. in Mexico expands the known distribution of the genus, indicating that its range may be broader than previously recognized. Future research should prioritize increasing molecular data, reassessing species with uncertain taxonomic status, and exploring new regions to further elucidate the diversity, evolutionary history, and biogeography of *Diaforobiotus*. This study underscores the critical role of integrative taxonomy in revealing the biodiversity of Mexican tardigrades, positioning Mexico as a significant centre for tardigrade research and highlighting its vital contribution to expanding our knowledge of these microscopic organisms in previously unexplored habitats.

Acknowledgments

This paper serves as a fulfillment of RAF-R for obtaining an MSc degree in the Posgrado en Ciencias Biológicas in Systematics, UNAM. RAF-R and BDL-S are grateful to Posgrado en Ciencias Biológicas and Instituto de Biología, Universidad Nacional Autónoma de México (UNAM). Also, RAF-R and BDL-S thank the Secretaría de Ciencia, Humanidades, Tecnología e Innovación (SECIHTI), for funding and the support of this research through a graduate scholarship. We thank the Programa de Apoyo a Estudiantes de Posgrado (PAEP). We also thank Pedro Mercado-Ruaro, from the Laboratorio de Botánica Estructural, for phase contrast photographs and allowing the implementation of the HotShot technique in the laboratory. We appreciate the services provided by the Laboratorio de Biología Molecular, the Laboratorio de Botánica Molecular and the Laboratorio de Microscopía y Fotografía de la Biodiversidad I of the Instituto de Biología, UNAM, as part of the Laboratorio Nacional de

Biodiversidad (LaNaBio). We are grateful for the technical support of Berenit Mendoza for assistance with PCM and SEM images, and of L. Cabrera-Martínez, N. López, and L. Márquez for their help with DNA extraction, amplification, and sequencing. We also thank Claudio Delgadillo-Moya, from Colección Nacional de Briofitas-MEXU, IBUNAM, for the identification of the moss. We thank J. Romero-Mendoza for genus identification. Special thanks to Sara Brandoli, Edoardo Massa, Lorena Rebecchi, Roberto Bertolani, Tiziana Altiero, Ilaria Giovannini, Federica Frigieri, from University of Modena and Reggio Emilia (UNIMORE) for all the facilities. The research leading to these results has received funding from the projects titled "Estudio de la diversidad de Tardígrados en la provincial del Eje Volcánico Transmexicano" and "Una aproximación integrativa para el estudio de la diversidad de escarabajos ambrosiales (Curculionidae: Scolytinae) de la Reserva de la Biósfera Volcán Tacaná: diversidad taxonómica, morfológica, genética y asociaciones simbióticas" in the frame program "Programa de Apoyo a Proyectos de Investigación e Innovación Tecnológica – UNAM" under Grant Nos. IA203122 and IN223924, respectively. D-CA, A-TF and EAR are members of SNII Secretaría de Ciencia, Humanidades, Tecnología e Innovación (SECIHTI).

Disclosure statement

No potential conflict of interest was reported by the author(s).

Author contributions

RAF-R prepared the draft and redaction of the manuscript and most figures, performed phylogenetic analyses and DNA extraction from moss and tardigrades, mounted the specimens and obtained measurements, prepared animals and eggs for SEM, and contributed to methodology and investigation.
L-SD prepared the draft of the manuscript, most figures and phylogenetic analyses, and redaction.
VJ conducted the delimitation of species,haplotype networking, and redaction.
CM conducted the delimitation of species, haplotype networking, phylogenetic analyses, software, and redaction.
GR inspected the slides, photographs, dichotomous key, and redaction.
D-CA performed manuscript editing, image editing, and proofreading of the type series.
A-TF and ER supervised the activities and provided funding acquisition, resources, conceptualization, and methodology.

Funding

This work was supported by the Programa de Apoyo a Proyectos de Investigación e Innovación Tecnológica-UNAM [IA203122].

ORCID

R. A. Flores-Romero http://orcid.org/0009-0004-1745-2713
D. López-Sandoval http://orcid.org/0009-0008-6347-4824
J. Vincenzi http://orcid.org/0009-0009-7924-4975
A. Dueñas-Cedillo http://orcid.org/0000-0002-9565-6621
E. A. Ruiz http://orcid.org/0000-0001-8738-8199
F. Armendariz-Toledano http://orcid.org/0000-0002-3130-4440

References

Altschul SF, Gish W, Miller W, Myers EW, Lipman DJ. 1990. Basic local alignment search tool. Journal of Molecular Biology 215(3):403–410. DOI: 10.1016/S0022-2836(05)80360-2.

Amezcua-Martínez C, Jimenez-Marín AR, Dueñas-Cedillo AR, Flores-Martínez JJ, Gómez-Lunar Z, Ruiz EA, Armendáriz-Toledano F, Bahder B. 2025. HotSHOT extraction is a fast, economical, and efficient method for obtaining tardigrade gDNA. Psyche: A Journal of Entomology 8887456(1):1–15. DOI: 10.1155/psyc/8887456.

Bartels P, Nelson DR. 2006. A large-scale, multihabitat inventory of the phylum Tardigrada in the Great Smoky Mountains National Park, USA: A preliminary report. Hydrobiologia 558(1):111–118. DOI: 10.1007/s10750-005-1405-9.

Bartels P, Nelson DR. 2007. An evaluation of species richness estimators for tardigrades of the Great Smoky Mountains National Park, Tennessee and North Carolina, USA. Journal of Limnology 66(1s):104–110. DOI: 10.4081/jlimnol.2007.s1.104.

Beasley C. 1972. Some tardigrades from Mexico. The Southwestern Naturalist 17(1):21–29. DOI: 10.2307/3669835.

Bertolani R, Guidetti R, Marchioro T, Altiero T, Rebecchi L, Cesari M. 2014. Phylogeny of Eutardigrada: New molecular data and their morphological support lead to the identification of new evolutionary lineages. Molecular Phylogenetics and Evolution 76:110–126. DOI: 10.1016/j.ympev.2014.03.006.

Camarda D, Massa E, Guidetti R, Lisi O. 2023. A new, simplified, drying protocol to prepare tardigrades for scanning electron microscopy. Microscopy Research and Technique 87(4):1–11. DOI: 10.1002/jemt.24460.
Clement M, Posada D, Crandall KA. 2000. TCS: A computer program to estimate gene genealogies. Molecular Ecology 29 (10):1657–1659. DOI: 10.1046/j.1365-294x.2000.01020.x.
Darriba D, Posada D, Kozlov A, Stamatakis A, Morel B, Flouri T. 2020. ModelTest-NG: A new and scalable tool for the selection of DNA and Protein evolutionary models. Molecular Biology and Evolution 37(1):291–294. DOI: 10.1093/molbev/msz189.
Degma P, Guidetti R. 2024. Actual checklist of Tardigrada species (2009–2024, 43th edition: 01-07-2024). Available: http://www.tardigrada.modena.unimo.it/miscellanea/Actual%20checklist%20of%20Tardigrada.pdf. Accessed November 2024 10.
Delgadillo-Moya C, Escolástico D, Hernández-Rodríguez E, Herrera-Paniagua P, Peña-Retes P, Juárez-Martínez C. 2022. Manual de briofitas. 3ra ed. Ciudad de México: Universidad Nacional Autónoma de México. México.
Dellaporta SL, Wood J, Hicks JB. 1983. A plant DNA minipreparation: Version II. Plant Molecular Biology Reporter 1(4):19–21. DOI: 10.1007/BF02712670.
dos Santos AM, Cabezas MP, Tavares AI, Xavier R, Branco M. 2016. tcsBU: A tool to extend TCS network layout and visualization. Bioinformatics 32(4):627–628. DOI: 10.1093/bioinformatics/btv636.
Dueñas-Cedillo A, García-Román J, Ruiz EA, Armendáriz-Toledano F. 2021. Species-specific cuticular phenotypes in Eutardigrada: A morphometric approach to analyze the variation of star-shaped pores in *Minibiotus* species. Diversity 13(7):307. DOI: 10.3390/d13070307.
Dueñas-Cedillo AR, Martínez-Méndez E, García-Román J, Armendáriz-Toledano F, Ruiz EA. 2020. Tardigrades from Iztaccíhuatl volcano (Trans-Mexican Volcanic Belt), with the description of *Minibiotus citlalium* sp. nov. (Eutardigrada: Macrobiotidae). Diversity 12(7):271. DOI: 10.3390/d1207027.
Dueñas-Cedillo AR, Venegas I, García-Román J, Jurado E, Cuellar-Rodríguez G, Villegas-Guzmán GA, Vargas-Mendoza CF, Ruiz EA, Armendáriz-Toledano F. 2024. Towards an inventory of Mexican tardigrades (Tardigrada): A survey on the diversity of moss tardigrades with an emphasis in conifer forests from the Valley of Mexico Basin. CheckList 20(2):471–498. DOI: 10.15560/20.2.471.
Fazekas AJ, Kuzmina ML, Newmaster SG, Hollingsworth PM. 2012. DNA barcoding methods for land plants. In: Kress W, Erickson D, editors. DNA barcodes: Methods in molecular biology. Vol. 858. Totowa, NJ: Humana Press. pp. 223–252. DOI:10.1007/978-1-61779-591-6_11.
Folmer O, Black M, Hoeh W, Lutz R, Vrijenhoek R. 1994. DNA primers for amplification of mitochondrial cytochrome c oxidase subunit I from diverse metazoan invertebrates. Molecular Marine Biology and Biotechnology 3(5):294–299.
Gámez N, Escalante T, Rodríguez-Tapia G, Linaje M, Morrone JJ. 2012. Caracterización biogeográfica de la Faja Volcánica Transmexicana y análisis de los patrones de distribución de su mastofauna. Revista Mexicana De Biodiversidad 83 (1):258–272. DOI: 10.22201/ib.20078706e.2012.1.786.
García-Román J, Dueñas-Cedillo AR, Cervantes-Espinoza M, Flores-Martínez JJ, Vargas-Mendoza CF, Ruíz EA, Armendáriz-Toledano F. 2022. A strategy to provide a present and future scenario of Mexican biodiversity of Tardigrada. Diversity 14(4):280. DOI: 10.3390/d14040280.
Gąsiorek P, Stec D, Zawierucha Z, Kristensen RM, Michalczyk Ł. 2018. Revision of *Testechiniscus* Kristensen, 1987 (Heterotardigrada: Echiniscidae) refutes the polar-temperate distribution of the genus. Zootaxa 4472(2):261–297. DOI: 10.11646/zootaxa.4472.2.3.
Gąsiorek P, Vončina K, Zając K, Michalczyc Ł. 2021. Phylogeography and morphological evolution of *Pseudoechiniscus* (Heterotardigrada: Echiniscidae). Scientific Reports 11(1):7606. DOI: 10.1038/s41598-021-84910-6.
Geospiza, Inc. 2004. FinchTV [software]. Disponible en. Available http://www.geospiza.com/Products/finchtv.shtml.
Glime JM. 2018. Tropics: Epiphyte Ecology, part 1. Chapter 8-3. In: Glime JM (Ed.), Bryophyte ecology. Vol. 4. Habitat and Role. Ebook sponsored by Michigan Technological University and the International Association of Bryologists. (pp. 8-3-4, 8-3-5) Last updated 22 July 2020 and http://digitalcommons.mtu.edu/bryophyte-ecology4/. Accessed 10 March 2024.
Guidetti R, Rebecchi L, Bertolani R, Jönsson KI, Kristensen RM, Cesari M. 2016. Morphological and molecular analyses on *Richtersius* (Eutardigrada) diversity reveal its new systematic position and lead to the establishment of a new genus and a new family within Macrobiotoidea. Zoological Journal of the Linnean Society 178(4):834–845. DOI: 10.1111/zoj.12428.
Guil N, Hortal J, Sánchez-Moreno S, Machordom A. 2009. Effects of macro and micro-environmental factors on the species richness of terrestrial tardigrades assamblages in an Iberian mountain environment. Landscape Ecology 24(3):375–390. DOI: 10.1007/s10980-008-9312-x.
Hart MW, Sunday J. 2007. Things Fall apart: Biological species form unconnected parsimony networks. Biology Letters 3 (5):509–512. DOI: 10.1098/rsbl.2007.0307.
Heinis F. 1911. Beitrag zur Kenntnis der zentralamericanischen Moosfauna. Revue Suisse de Zoologie 19:253–266. DOI: 10.5962/bhl.part.29917.
Hoang DT, Chernomor O, von Haeseler A, Minh BQ, Vinh LS. 2018. UFBoot2: Improving the ultrafast bootstrap approximation. Molecular Biology and Evolution 35(2):518–522. DOI: 10.1093/molbev/msx281.
Hoffman A, Jiménez ML. 1994. Tardígrados en México. Anales del Instituto de Biología, Universidad Nacional Autónoma de México. Serie Zoología 65(2):297–301.

Johansson C, Miller WR, Linde ET, Adams BJ, Boreliz-Alvarado E. 2013. Tardigrades of Alaska: Distribution patterns, diversity and species richness. Polar Research 32(1):1–11. DOI: 10.3402/polar.v32i0.18793.

Jørgensen A, Kristensen RM, Møbjerg N. 2018. Phylogeny and integrative taxonomy of Tardigrada. Phylogeny and integrative taxonomy of Tardigrada. Handbook of Environmental Chemistry 1:95–114. DOI: 10.1007/978-3-319-95702-9_3.

Jørgensen M, Kristensen RM. 1991. Meiofuna investigations from Igloolik, N.W.T. Artic Canada. In: Jørgensen M, editor. Artic biology course 1989 Igloolik Northwest Territories Canada. Copenhagen: Zoological Museum, University of Copenhagen. pp. 61–80.

Kaczmarek Ł, Bartołomiej G, Wełnicz W, Michalczyk Ł. 2011a. Ecological factors determining Tardigrada distribution in Costa Rica. Journal of Zoological Systematics & Evolutionary Research 49(s1):78–83. DOI: 10.1111/j.1439-0469.2010.00603.x.

Kaczmarek Ł, Cytan J, Zawierucha K, Diduszko D, Michalczyk Ł. 2014a. Tardigrades from Peru (South America), with descriptions of three new species of Parachela. Zootaxa 3790(2):357–379. DOI: 10.11646/zootaxa.3790.2.5.

Kaczmarek Ł, Diduszko D, Michalczyk L. 2011b. New records of Mexican Tardigrada. Revista Mexicana De Biodiversidad 82 (4):1324–1327. DOI: 10.22201/ib.20078706e.2011.4.754.

Kaczmarek Ł, Michalczyk Ł. 2017. The *Macrobiotus hufelandi* group (Tardigrada) revisited. Zootaxa 4343(1):101–123. DOI: 10.11646/zootaxa.4363.1.4.

Kaczmarek Ł, Michalczyk Ł, Mcinnes SJ. 2016. Annotated zoogeography of non-marine Tardigrada. Part III: North America and Greenland. Zootaxa 4203:1–249.

Kalyaanamoorthy S, Minh BQ, Wong TKF, von Haeseler A, Jermiin LS. 2017. ModelFinder: Fast model selection for accurate phylogenetic estimates. Nature Methods 14(6):587–589. DOI: 10.1038/nmeth.4285.

Kathman RD. 1990. Some tardigrades from Colorado, with a description of a new species of *Macrobiotus* (Macrobiotudae: Eutardigrada). Proceedings of the Biological Society of Washington 103(2):300–303.

Katoh K, Misawa K, Kuma K, Miyata T. 2002. MAFFT: A novel method for rapid multiple sequence alignment based on fast fourier transform. Nucleic Acids Research 30(14):3059–3066. DOI: 10.1093/nar/gkf436.

Katoh K, Rozewicki J, Yamada KD. 2019. MAFFT online service: Multiple sequence alignment, interactive sequence choice and visualization. Briefings in Bioinformatics 20(4):1160–1166. DOI: 10.1093/bib/bbx108.

Kayastha P, Berdi D, Mioduchowska M, Gawlak M, Łukasiewicz A, Gołdyn B, Jedrzejewski S, Kaczmarek Ł. 2020. Description and molecular characterization of *Richtersius ziemowiti* sp. nov. (Richtersiidae) from Nepal (Asia) with evidence of heterozygous point mutation events in the 28S rRNA. Annales Zoologici 70(3):381–396. DOI: 10.3161/00034541ANZ2020.70.3.010.

Massa E, Vecchi M, Calhim S, Choong H. 2024. First records of limnoterrestrial tardigrades (Tardigrada) from Haida Gwaii, British Columbia, Canada. European Zoological Journal 91(1):1–20. DOI: 10.1080/24750263.2023.2288824.

Mastretta-Yanes A, Moreno-Letelier A, Piñero D, Jorgensen TH, Emerson B. 2015. Biodiversity in the Mexican highlands and the interaction of geology, geography and climate within the Trans-Mexican volcanic Belt. Journal of Biogeography 42(9):1586–1600. DOI: 10.1111/jbi.12546.

Maucci W. 1982. Sulla presenza in Italia di *Cornechiniscus holmeni* (Petersen, 1951), e descrizione di *Macrobiotus hyperonyx* sp. nov. (Tardigrada). Bollettino Del Museo Civico Di Storia Naturale Di Verona 9:175–179.

McInnes S, Convey S. 2005. Tardigrade fauna of the South Sandwich Islands, maritime Antartic. Zootaxa 1058(1):43–29. DOI: 10.11646/zootaxa.1058.1.3.

Meyer HA. 2001. Tardigrada of Luoisiana and Arkansas, United States of America. Zoologischer Anzeiger 240(3–4):471–474. DOI: 10.1078/0044-5231-00056.

Meyer HA, Hinton JG. 2012. New water bear records (Phylum Tardigrada) from the Pacific Northwest of North America. The pan-Pacific Entomologist 88(3):304–310. DOI: 10.3956/2012-06.1.

Michalczyk Ł, Kaczmarek Ł. 2006. *Macrobiotus huziori*, a new species of Tardigrada (Eutardigrada: Macrobiotidae) from Costa Rica (Central America). Zootaxa 1169(1):47–59. DOI: 10.11646/zootaxa.1169.1.3.

Michalczyk Ł, Kaczmarek Ł. 2013. The Tardigrada register: A comprehensive online data repository for tardigrade taxonomy. Journal of Limnology 72(1s):175–181. DOI: 10.4081/jlimnol.2013.s1.e22.

Michalczyk Ł, Wełnicz W, Frohme M, Kaczmarek Ł. 2012. Redescriptions of three *Milnesium* Doyère, 1840 taxa (Tardigrada: Eutardigrada: Milnesiidae), including the nominal species for the genus. Zootaxa 3154(1):1–20. DOI: 10.11646/zootaxa.3154.1.1.

Minh B, Schmidt H, Chernomor O, Schrempf D, Woodhams M, von Haeseler A, Lanfear R. 2020. IQ-TREE 2: New models and efficient methods for phylogenetic inference in the genomic Era. Molecular Biology and Evolution 37(5):1530–1534. DOI: 10.1093/molbev/msaa015.

Mironov SV, Dabert J, Dabert M. 2012. A new feather mite species of the genus *Proctophyllodes* Robin, 1877 (Astigmata: Proctophyllodidae) from the long-tailed Tit *Aegithalos caudatus* (Passeriformes: Aegithalidae): Morphological description with DNA barcode data. Zootaxa 3253(1):54–61. DOI: 10.11646/zootaxa.3253.1.2.

Montero-Pau J, Gómez A, Muñoz J. 2008. Application of an inexpensive and high-troughput genomic DNA extraction method for the molecular ecology of zooplanktonic diapausing eggs. Limnology and Oceanographyc Methods 6 (6):218–222. DOI: 10.4319/lom.2008.6.218.

Moreno-Talamantes A, León-Espinosa GA. 2019. Nuevo Registro De *Diaforobiotus islandicus* (Richters, 1904) (Eutardigrada: Richtersiusiidae) Para México. Árido-Ciencia 6(1):5–12.

Moreno-Talamantes A, León-Espinosa GA, García-Aranda MA, Flores-Maldonado JJ, Kaczmarek L. 2020. The genus *Milnesium* Doyère, 1840 in Mexico with description of a new species. Annales Zoologici 70(4):467–486. DOI: 10.3161/00034541ANZ2020.70.4.001.

Moreno-Talamantes A, Roszkowska M, Garcia-Aranda MA, Flores-Maldonado JJ, Ł K. 2019. Current knowledge on Mexican tardigrades with a description of milnesium cassandrae sp. nov. (Eutardigrada: Milnesiidae) and discussion on the taxonomic value of dorsal pseudoplates in the genus milnesium doyere, 1840. Zootaxa 4691:501–524. DOI: 10.11646/zootaxa.4691.5.5.

Morrone JJ. 2005. Toward a synthesis of Mexican biogeography. Revista Mexicana De Biodiversidad 76(2):207–252. DOI: 10.22201/ib.20078706e.2005.002.303.

Morrone JJ. 2010. Fundamental biogeographic patterns across the Mexican transition zone: An evolutionary approach. Ecography 33(2):355–361. DOI: 10.1111/j.1600-0587.2010.06266.x.

Murray J 1910. Tardigrada. Reports on the Scientific investigations of the British Antarctic expedition 1907-1909. Reports on the Scientific investigations, vol. I: Biology, part V: Tardigrada.

Nelson DR. 1982. Developmental Biology of the Tardigrada. In: Harrison RA, Cowden DC, editors. Developmental biology of freshwater invertebrates. New York: Alan R. Liss. pp. 363–398.

Nelson DR, Bartels PJ, Fegley SR. 2019. Environmental correlates of tardigrade community structure in mosses and lichens in the Great Smoky Mountains National Park (Tennessee and North Carolina, USA). Zoological Journal of the Linnean Society XX:1–12. DOI: 10.1093/zoolinnean/zlz043.

Nichols PB, Nelson D, Garey JR. 2006. A family level analysis of tardigrade phylogeny. Hidrobiologia 558(1):53–60. DOI: 10.1007/s10750-005-1414-8.

Nowak B, Stec D. 2018. An integrative description of *Macrobiotus hannae* sp. nov. (Tardigrada: Eutardigrada: Macrobiotidae: *Hufelandi* group) from Poland. Turkish Journal of Zoology 42:269–286. DOI: 10.3906/zoo-1712-31.

Pérez-Pech WA, Anguas-Escalante A, Cutz-Pool LQ, Guidetti R. 2017. *Doryphoribius chetumalensis* sp. nov. (Eutardigrada: Isohypsibiidae) a new tardigrade species discovered in an unusual habitat of urban areas of Mexico. Zootaxa 4344 (2):347–352. DOI: 10.11646/zootaxa.4344.2.9.

Pilato G. 2024. Discussion on the morphological and molecular data used in the study of tardigrade systematics. Biodiversity Journal 15(4):935–955. DOI: 10.31396/Biodiv.Jour.2024.15.4.935.955.

Pilato G, Binda MG. 2010. Definition of families, subfamilies, genera and subgenera of the Eutardigrada, and keys to their identification. Zootaxa 2404(1):1–54. DOI: 10.5281/zenodo.194138.

Pogwizd J, Stec D. 2022. An integrative description of a new *Richtersius* species from Greece (Tardigrada: Eutardigrada: Richtersiusidae). Acta Zoologica Academiae Scientiarum Hungaricae 68(1):1–21. DOI: 10.17109/AZH.68.1.1.2022.

Puillandre N, Brouillet S, Achaz G. 2020. ASAP: Assemble species by automatic partitioning. Molecular Ecology Resources 21(2):609–620. DOI: 10.1111/1755-0998.13281.

Rambaut A, Drummond AJ, Xie D, Baele G, Suchard MA. 2018. Posterior summarisation in Bayesian phylogenetics using Tracer 1.7. Systematic Biology 67(5):901–904. DOI: 10.1093/sysbio/syy032.

Richters F. 1904. Islandische Tardigraden. Zoologischer Anzeiger 28:373–377.

Ronquist F, Huelsenbeck JP. 2003. MrBayes 3: Bayesian phylogenetic inference under mixed models. Bioinformatics 19 (12):1572–1574. DOI: 10.1093/bioinformatics/btg180.

Schill RO. 2008. Water bears: The biology of tardigrades. Zoological monographs. Vol. 2. Berlin: Springer.

Schneider CA, Rasband WS, Eliceiri KW. 2012. NIH image to ImageJ: 25 years of image analysis. Nature Methods 9(7):671–675. DOI: 10.1038/nmeth.2089.

Schuster RO, Toftner EC 1982. Dominican Republic Tardigrada. Proceedings of Third International Symposium on the Tardigrada. East University Press, Johnson City, Tennessee 37614–0002, USA, 221–236.

Séméria Y. 1985. Deux Nouvelles forms de Tardigrades du Nicaragua: *Echiniscus maesi* s. sp. (Heterotardigrada, Echiniscoidea, Echiniscidea) et *Macrobiotus islandicus nicaraguensis* n. ssp. (Eutardigrada, Macrobiotidae). Comptes Rendus de l'Académie Des Sciences 300:9–11.

Séméria Y, Elin D. 1989. Les tardigrades du Groenland. Resultats de la 2e expedition du G.E.C.R.P. au Scoresbysund (cote orietale - 1985. Extrait du Bulletin Mensuel de la Société Linnéenne de Lyon 58(4):124–134. DOI: 10.3406/linly.1989.10870.

Stamatakis A. 2014. RAxML version 8: A tool for phylogenetic analysis and post-analysis of large phylogenies. Bioinformatics 30(9):1312–1313. DOI: 10.1093/bioinformatics/btu033.

Stec D. 2023. Integrative taxonomy helps to revise systematics and questions the purported cosmopolitan nature of the type species within the genus *Diaforobiotus* (Eutardigrada: Richtersiusidae). Organisms Diversity & Evolution 23 (2):309–328. DOI: 10.1007/s13127-022-00592-6.

Stec D, Arakawa K, Michalczyk Ł. 2018. An integrative description of *Macrobiotus shonaicus* sp. nov. (Tardigrada: Macrobiotidae) from Japan with notes on its phylogenetic position within the *hufelandi* group. PLOS ONE 13(2): e0192210. DOI: 10.1371/journal.pone.0192210.

Stec D, Gąsiorek P, Morek W, Kosztyla P, Zawierucha K, Michno K, Kaczmarek Ł, Prokop ZM, Michalczyk Ł. 2016. Estimating optimal sample size for tardigrade morphometry. Zoological Journal of the Linnean Society 178(4):1–9. DOI: 10.1111/zoj.12404.

Stec D, Krzywańsk Ł, Arakawa K, Michalczyk Ł. 2020a. A new redescription of *Richtersius coronifer*, supported by transcriptome, provides resources for describing concealed species diversity within the monotypic genus *Richtersius* (Eutardigrada). Zoological Letters 6(1):2. DOI: 10.1186/s40851-020-0154-y.

Stec D, Morek W. 2022. Reaching the monophyly: Re-evaluation of the enigmatic species *Tenuibiotus hyperonyx* (Maucci, 1983) and the genus *Tenuibiotus* (Eutardigrada). Animals 12(3):404. DOI: 10.3390/ani12030404.

Stec D, Vecchi M, Maciejowski W, Michalczyk Ł. 2020b. Resolving the systematics of richtersiidae by multilocus phylogeny and an integrative redescription of the nominal species for the genus *Crenubiotus* (Tardigrada). Scientific Reports 10 (1):19418. DOI: 10.1038/s41598-020-75962-1.

Stec D, Zawierucha K, Michalczyk Ł. 2017. An integrative description of *Ramazzottius subanomalus* (Biserov, 1985 (Tardigrada) from Poland. Zootaxa 4300(3):403–420. DOI: 10.11646/zootaxa.4300.3.4.

Tamura K, Stecher G, Kumar S. 2021. MEGA11: Molecular evolutionary genetics analysis version 11. Molecular Biology and Evolution 38(7):3022–3027. DOI: 10.1093/molbev/msab120.

Templeton AR, Crandall KA, Sing CF. 1992. A cladistic analysis of phenotypic associations with haplotypes inferred from restriction endonuclease mapping and DNA sequence data. III. Cladogram estimation. Genetics 132(2):619–633. DOI: 10.1093/genetics/132.2.619.

Tumanov DV. 2005. Two new species of *Macrobiotus* (Eutardigrada, Macrobiotidae) from Tien Shan (Kirghizia), with notes on *Macrobiotus tenuis* group. Zootaxa 1043(1):33–46. DOI: 10.1646/ZOOTAXA.1043.1.3.

Vaidya G, Lohman DJ, Meier R. 2011. SequenceMatrix: Concatenation software for the fast assembly of multi-gene datasets with character set and codon information. Cladistics 27(2):171–180. DOI: 10.1111/j.1096-0031.2010.00329.x.

Zawierucha K, Węgrzyn M, Ostrowska M, Wietrzyk P. 2017. Tardigrada in Svalbard lichens: Diversity, densities and habitat heterogeneity. Polar Biology 40(7):1385–1392. DOI: 10.1007/s00300-016-2063-2.

Zhang J, Kapli P, Pavlidis P, Stamatakis A. 2013. A general species delimitation method with applications to phylogenetic placements. Bioinformatics 29(22):2869–2876. DOI: 10.1093/bioinformatics/btt499.